



TOHOKU
UNIVERSITY



14th European Conference on Applied Superconductivity
1st-5th September 2019, SEC, Glasgow

Superconductors in High Magnetic Fields - Now and the future -

Satoshi Awaji

High Field Laboratory for Superconducting Materials
(HFLSM),
Institute for Materials Research, Tohoku University





TOHOKU
UNIVERSITY

Collaborators

2

Tohoku University:

T. Okada, K. Sakai, H. Misaizu, K. Takahashi, A. Badel



Nagoya University

Y. Tsuchiya, Y. Ichino, Y. Yoshida



Kyusyu Inst. Technol.

T. Horide, K. Matsumoto



Tokai University

H. Oguro



KEK

M. Sugano, T. Nakamoto, T. Ogitsu



NIMS

G. Nishijima

FURUKAWA ELECTRIC



Furukawa:

M. Sugimoto, H. Tsubouchi, H. Sakamoto,

Furukawa-SuperPower:

S. Yamano, T. Fukushima



JASTEC-Kobe Steel:

S. Kawashima, K. Saito, Y. Fukumoto



Fujikura:

S. Fujita, S. Muto, Y. Iijima, M. Daibo



Super OX Japan:

V. Petrykin, M. Gaifullin, U. Pyot, S. Lee



Special Thanks

SuNAM: H. Lee, S. Moon

Shanghai Supercond. Techn.: Y. Yamada





TOHOKU
UNIVERSITY

3

Superconductors in High Magnetic Fields - Now and the future -

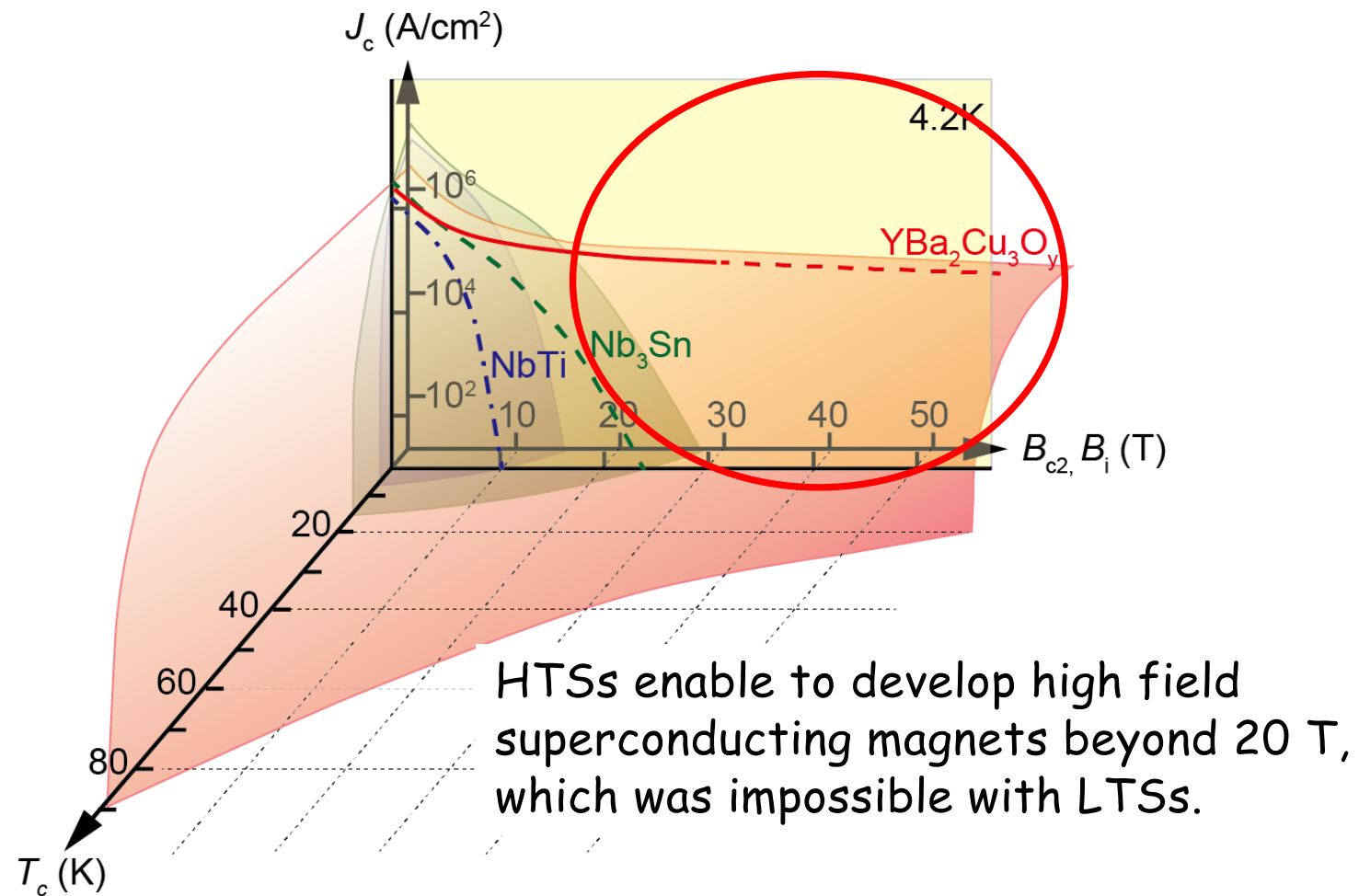
Contents

1. Status of practical superconductors
2. Nb_3Sn
3. Bi-Sr-Ca-Cu-O ($\text{Bi}_2\text{Sr}_2\text{Ca}_2\text{Cu}_3\text{O}_y$, $\text{Bi}_2\text{Sr}_2\text{Ca}_1\text{Cu}_2\text{O}_y$)
4. $\text{REBa}_2\text{Cu}_3\text{O}_y$
5. Fe-based Superconductor (IBS)
6. To develop high field superconducting magnet
7. Summary





Critical surface of practical SC



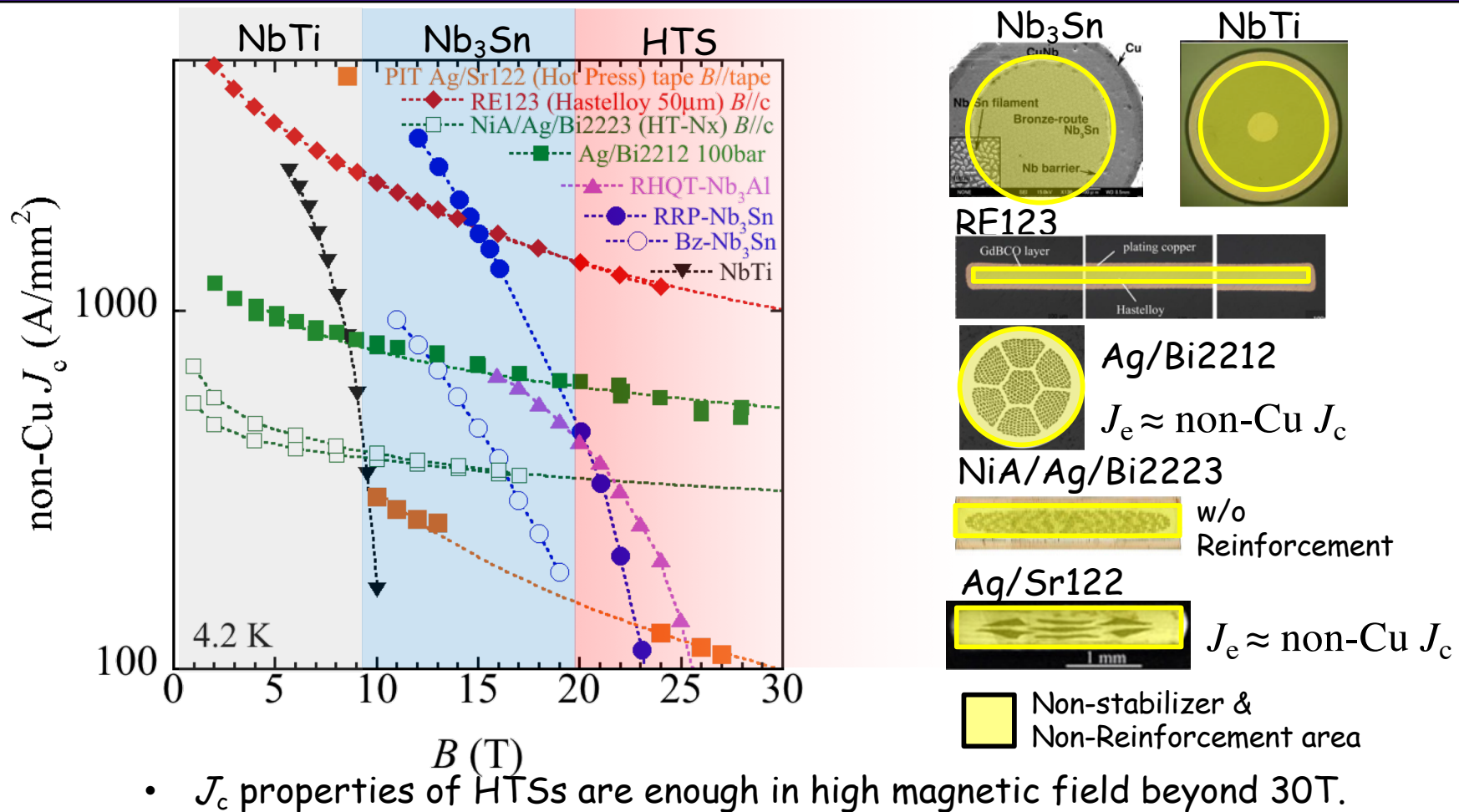


Key properties in High Field Superconductors

- Non-Cu J_c in high magnetic field
 - Introduction of flux pinning center to increase layer J_c
 - Increase volume fraction SC
- Stress/strain effect on J_c
 - Understand and control strain effects on J_c
 - Reinforcement with high strength materials.



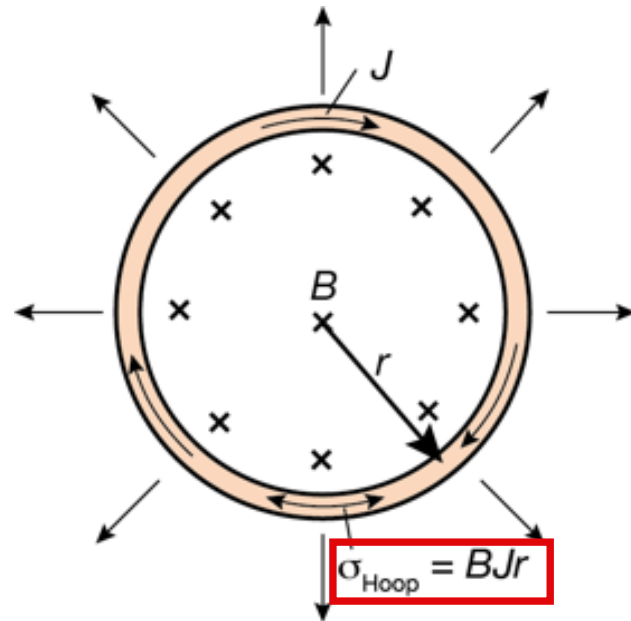
Non-Cu J_c (non stabilizer J_c)



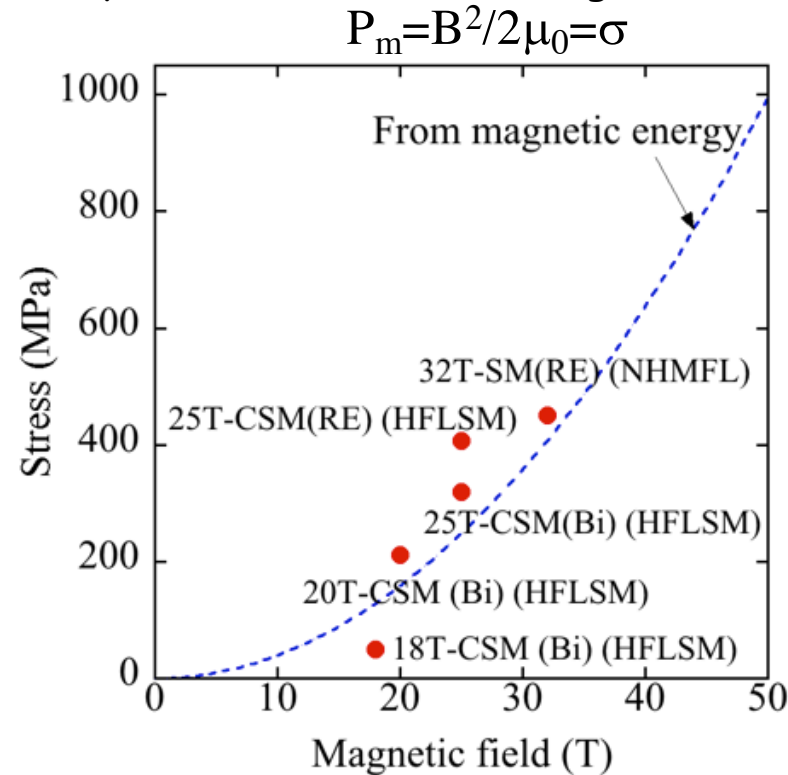


Mechanical stress in the magnet

Hoop stress from electromagnetic forces



Equivalent stress from magnetic energy

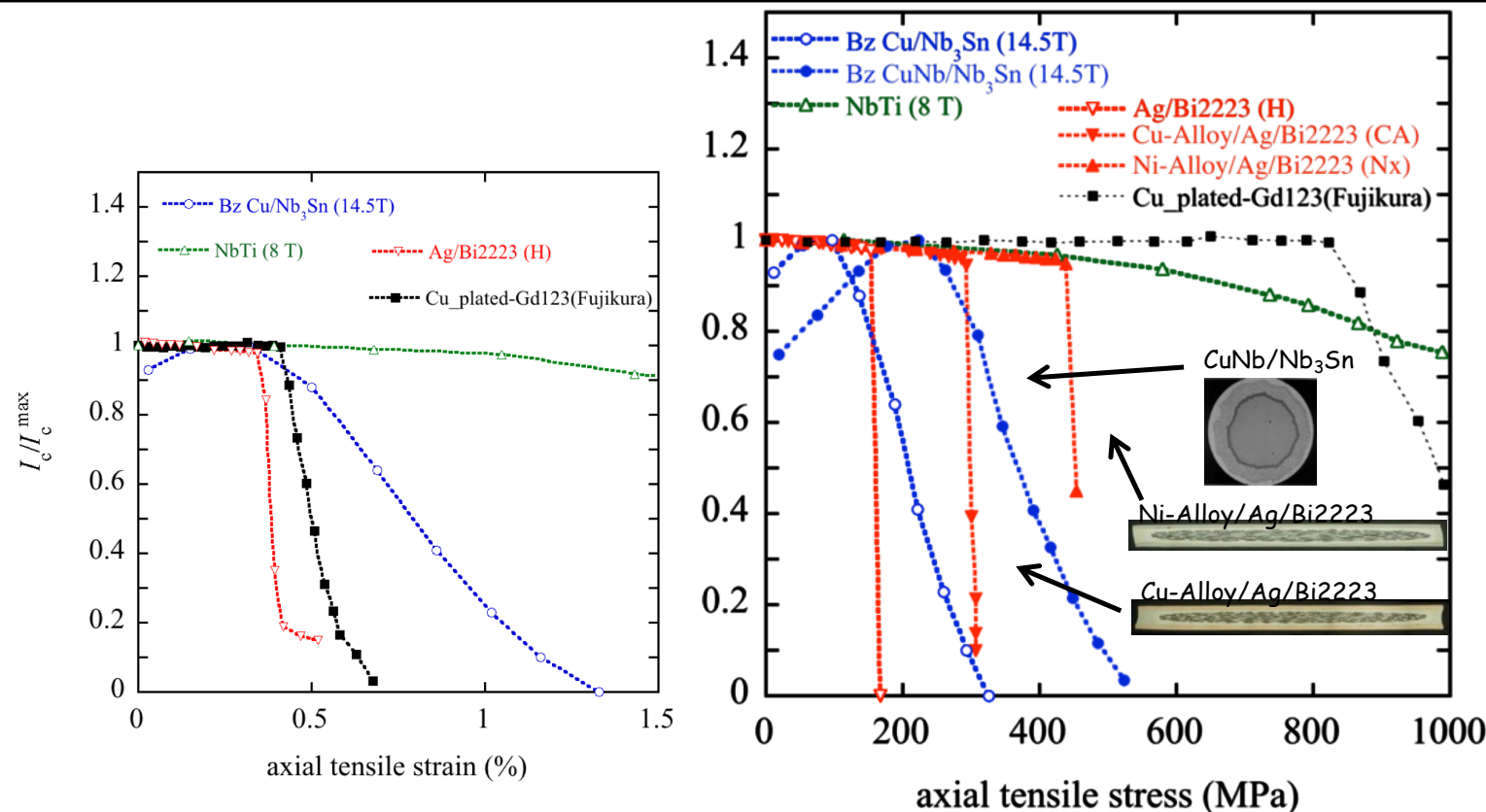


J. Ekin, Experimental Techniques for Low-Temperature Measurements, Oxford Univ. Press, 2006.

Eletoromechanical properties (stress/strain dependence of J_c) are important for high field magnets as well as in-field J_c .



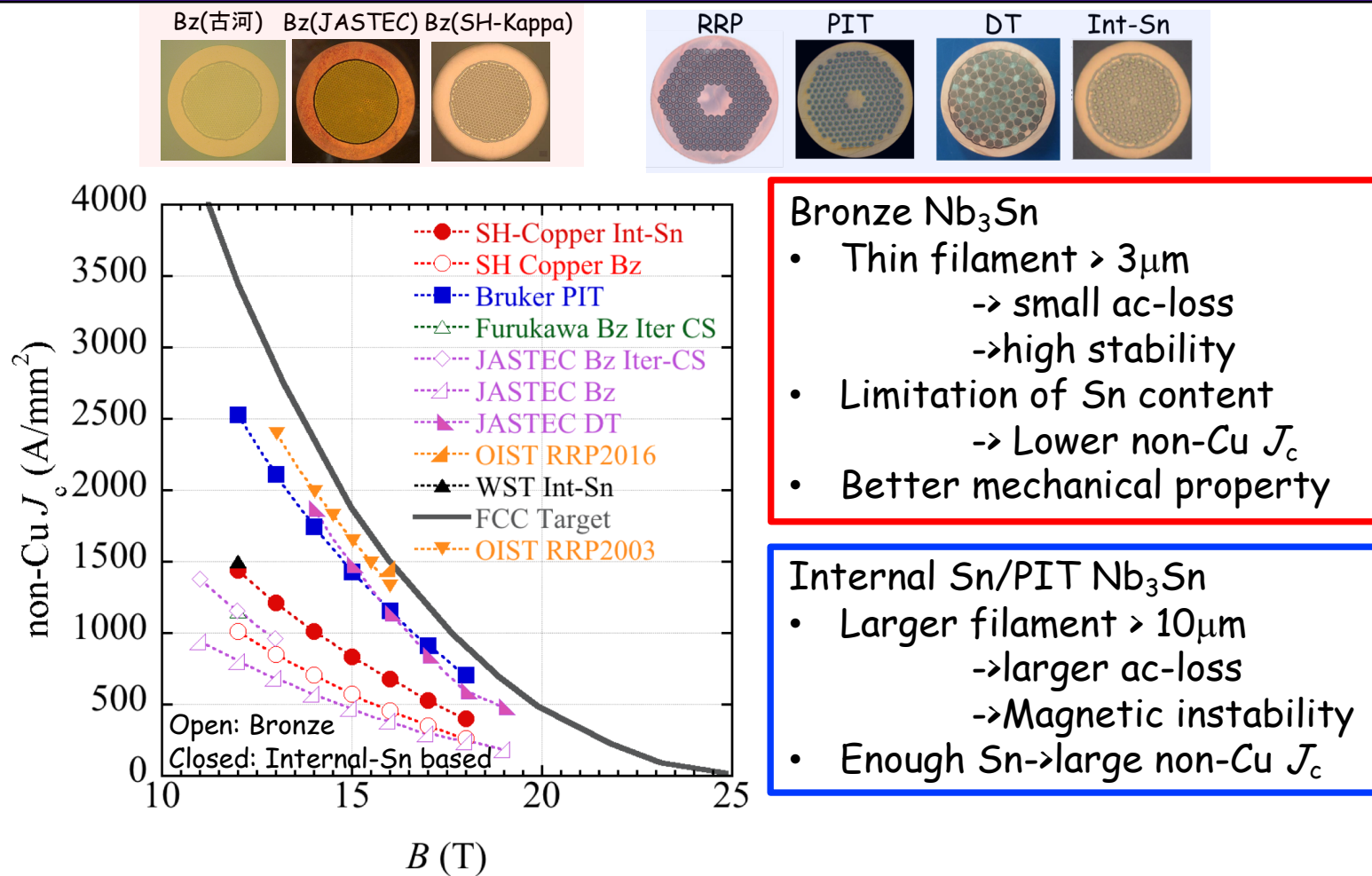
Importance of mechanical strength



- Alloy SC NbTi has broad strain dependence.
- Strain limits of most superconductors are 0.3-0.5%.
- Reinforcement is necessary for high field magnet.



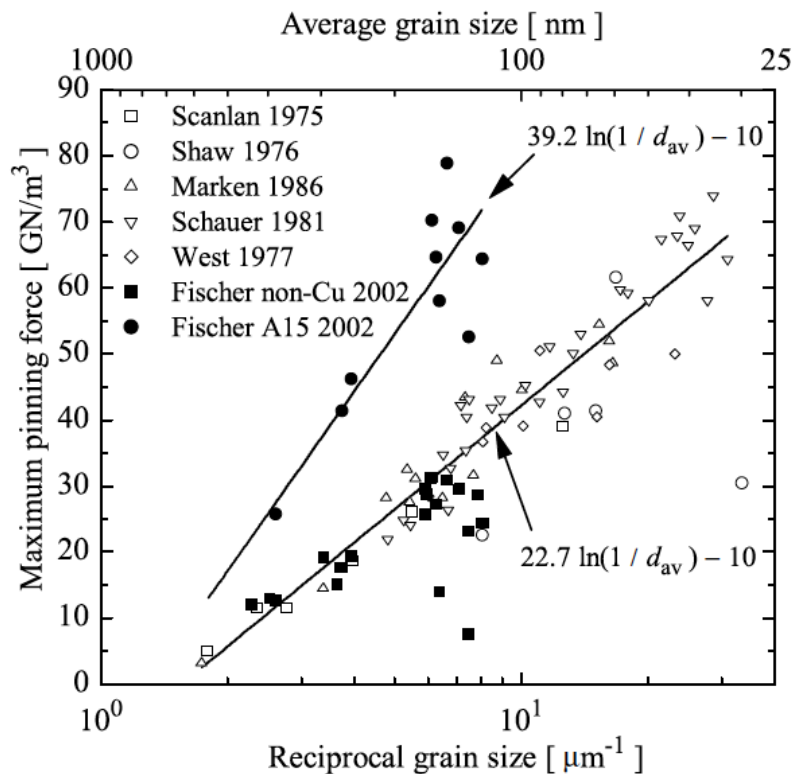
Practical Nb₃Sn wires





Flux pinning of Nb_3Sn - grain boundary -

10



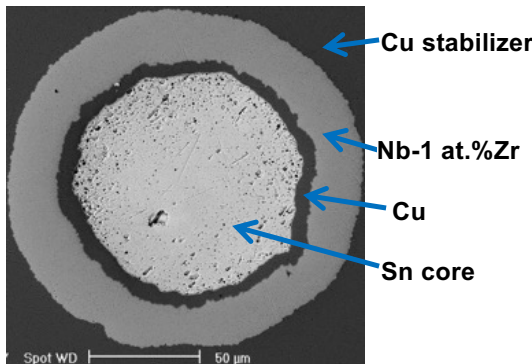
Dominant flux pinning center in Nb_3Sn wires is grain boundary!

Figure 10. Maximum pinning force as function of reciprocal grain size, after Fischer [89]. (*Adapted with kind permission of C M Fischer*).

Godeke, SuST 19 (2006) R68

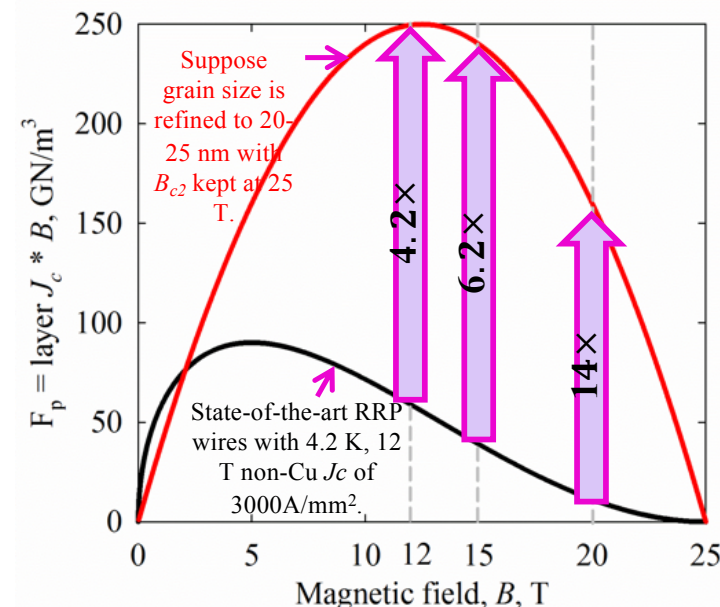
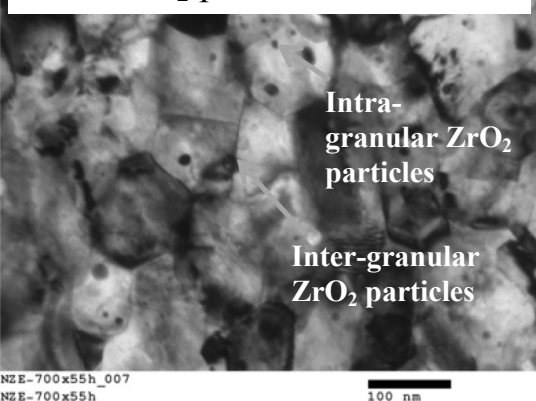


Improve flux pinning in Nb₃Sn wires



X. Xu et al., Appl. Phys. lett. **104**, 082602

Note ZrO₂ particles 10 nm OD



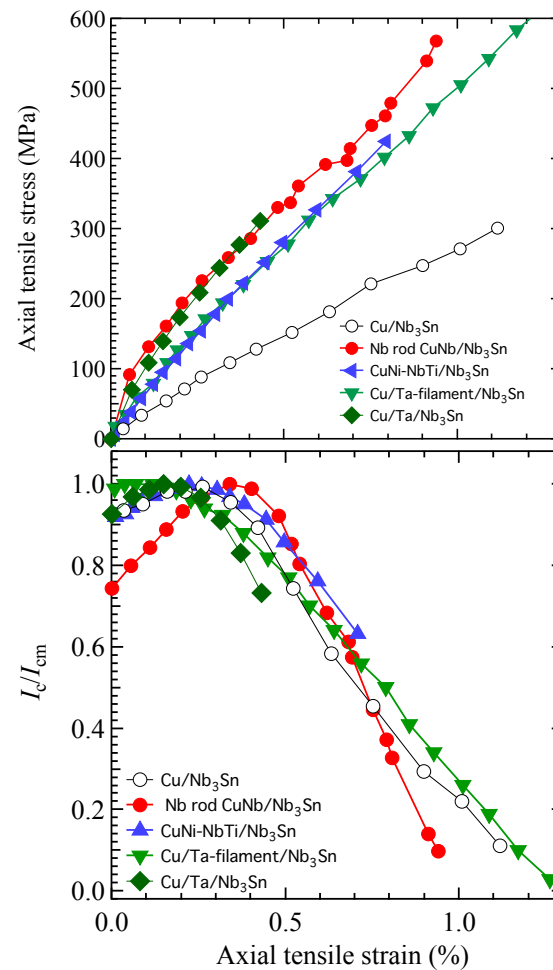
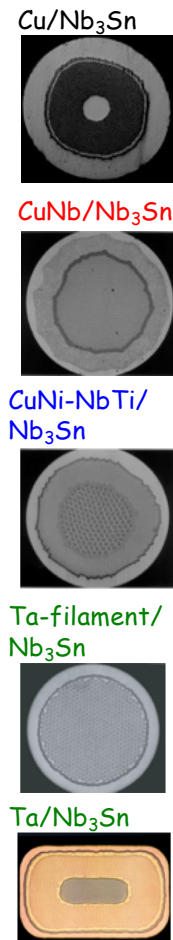
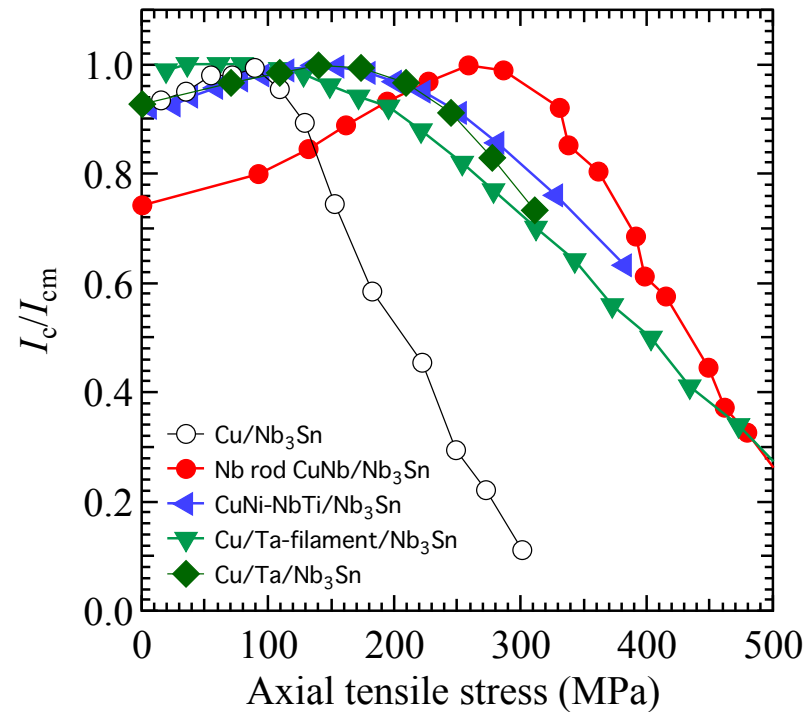
How do ZrO₂ particles refine Nb₃Sn grain size?

- **Impede Grains coarsening:** distinct gradients in grain size.
- **Be nucleation centers:** newly-formed grains in the internal oxidation samples are smaller.

M. Sumption, FCC week 2016 slides



High strength Nb₃Sn



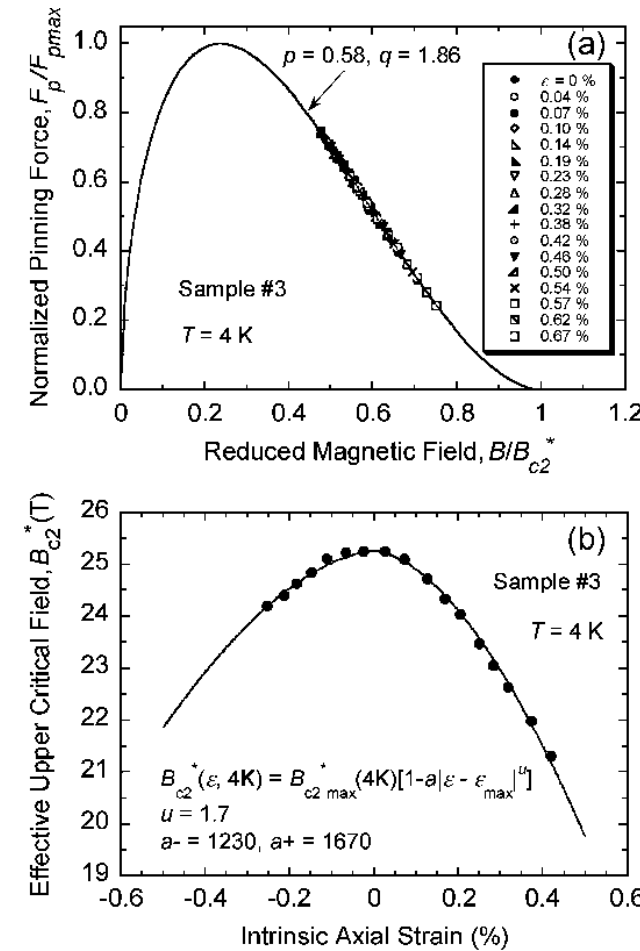
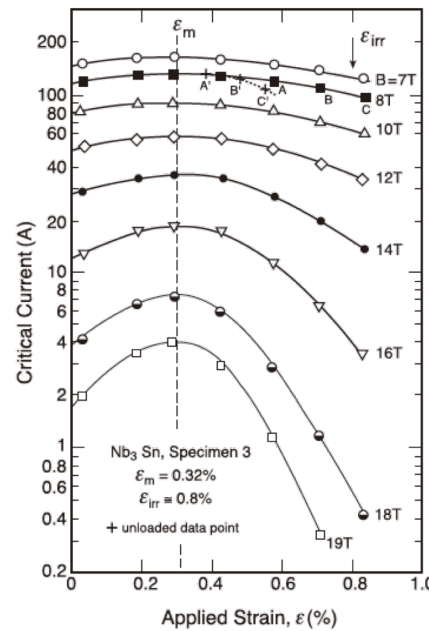
- From application view point,
Stress is important.
- From material view point,
Strain controls property.
- Steep SS curve reduces strain



Strain dependence of Nb₃Sn

- Thermal strain due to the composite
- J_c peak at thermal strain
- Scaling of $J_c(\varepsilon)$ curves by $B_{c2}(\varepsilon)$

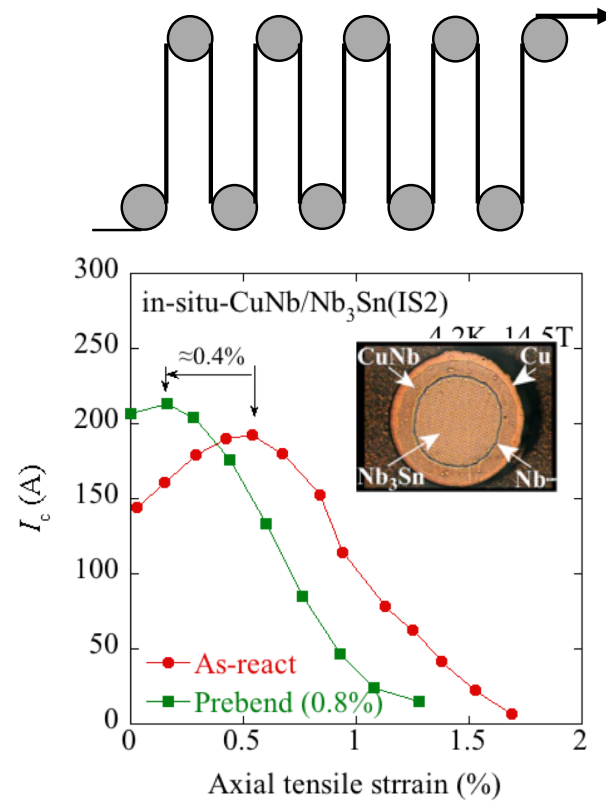
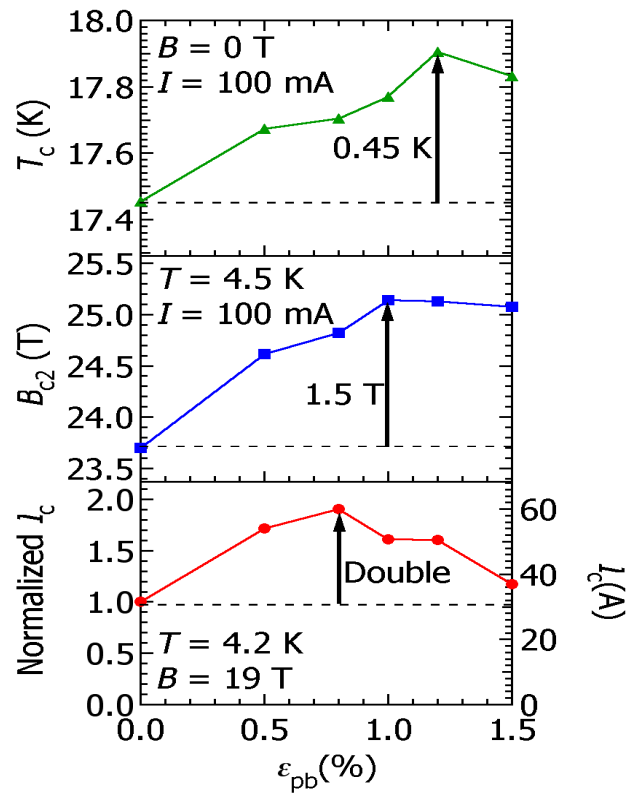
$$\frac{J_c}{J_{cm}} = \left[\frac{B_{c2}^*(\varepsilon)}{B_{c2m}^*} \right]^{n-q} \left[\frac{1 - B/B_{c2}^*(\varepsilon)}{1 - B/B_{c2m}^*} \right]^q$$





Effect of internal strains —pre-bending treatment—

14



Prebending (repeated bending) improves all superconducting parameters because of a change of residual strain state.



Angular dependence of internal strain ($\text{CuNb}/\text{Nb}_3\text{Sn}$)

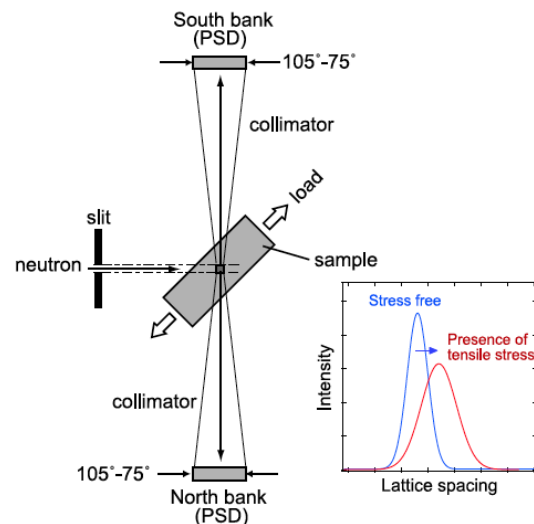


Figure 5. Experimental setup for the TOF diffraction at TAKUMI [6].

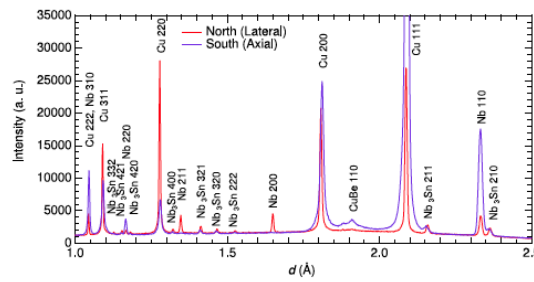
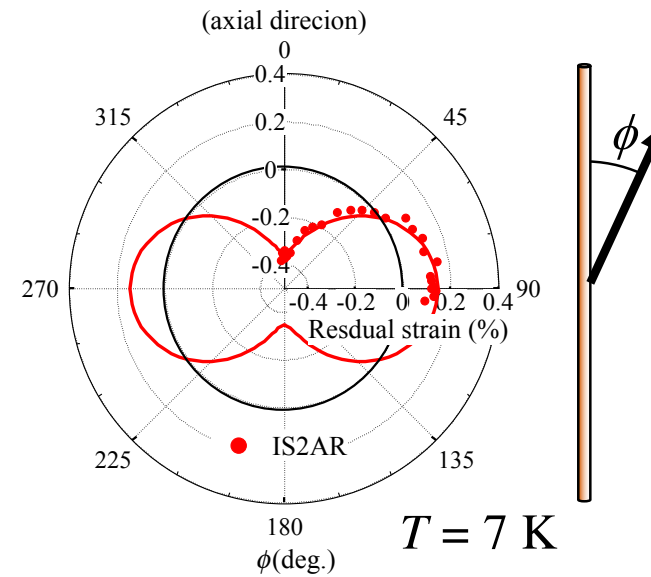
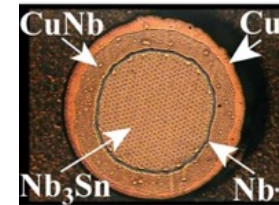


Figure 6. Typical diffraction pattern of $\text{Cu}20\%\text{Nb}/(\text{Nb}, \text{Ti})_3\text{Sn}$ wires measured by the TOF method at TAKUMI.

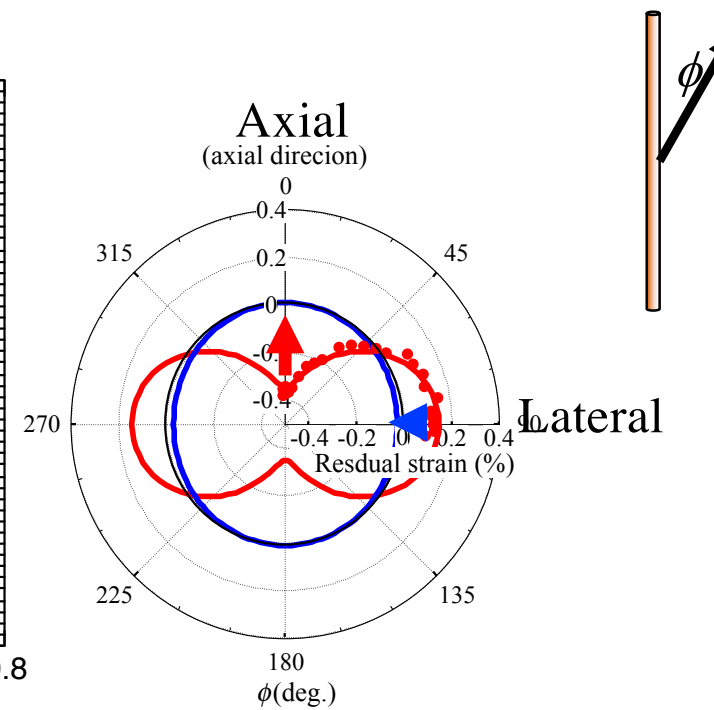
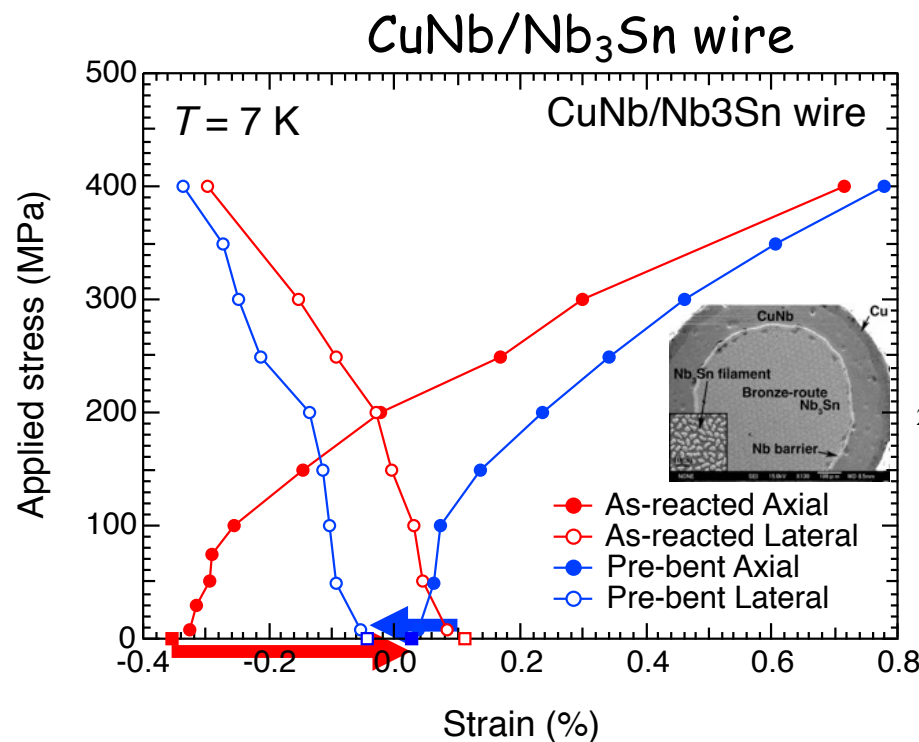


$$\varepsilon(\theta) = \sqrt{\left(1 + \varepsilon_z\right)^2 \sin^2 \theta + \left(1 + \varepsilon_r\right)^2 \cos^2 \theta} - 1$$

S. Awaji et al, SuST 23 (2010) 105010, SuST 26 (2013)073001.



Effect of prebending

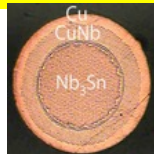


- ✓ Improve J_c and mechanical property by pre-bending process due to the plastic deformation and work hardening of CuNb.
- ✓ Improve J_c^{\max} due to the change of 3D strain

Advanced technology of Nb_3Sn conductor for 25T-CSM

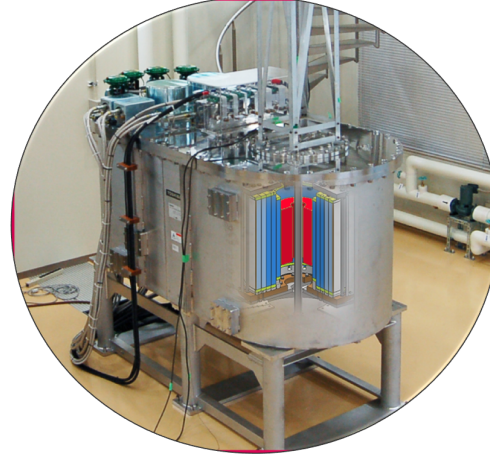


High strength (CuNb/Nb₃Sn)



Oguro et al., SuST. 26
 (2013) 094002.

25T-CSM

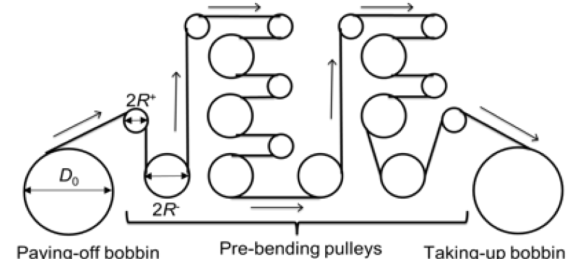


Rutherford cable



Sugimoto et al., IEEE TAS., 25
 (2015) 6000605.

Pre-bending (0.5%)



React & Wind (Strain management)

Oguro et al., SuST. 29 (2016) 084004.

LTS: $\phi 300\text{mm}-14\text{T}@854\text{A}$

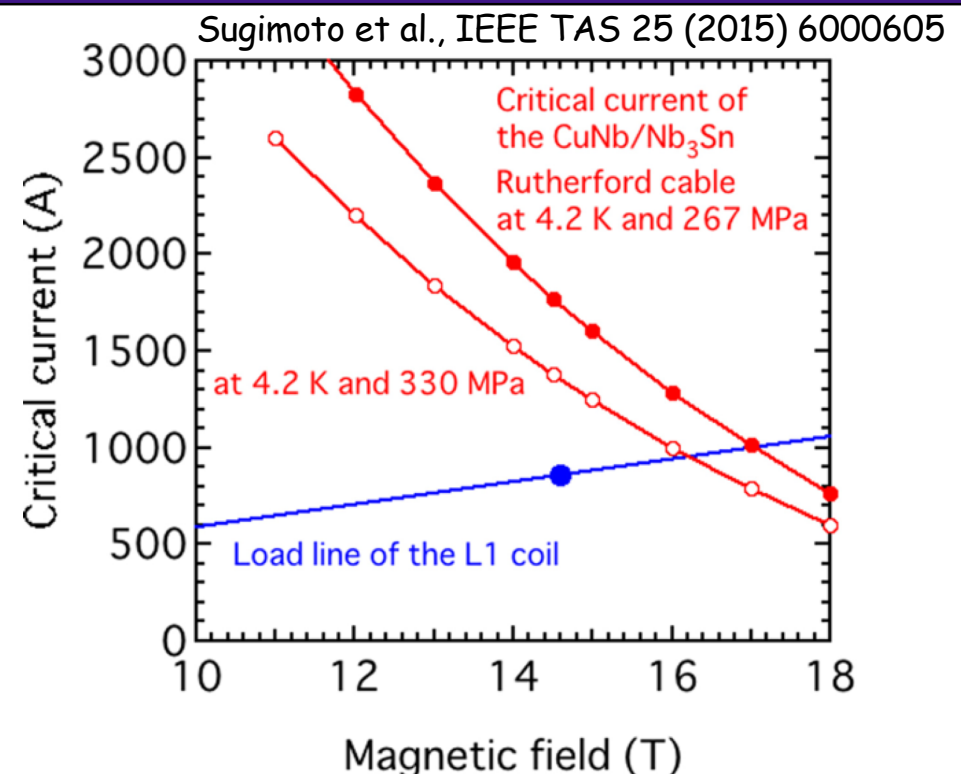
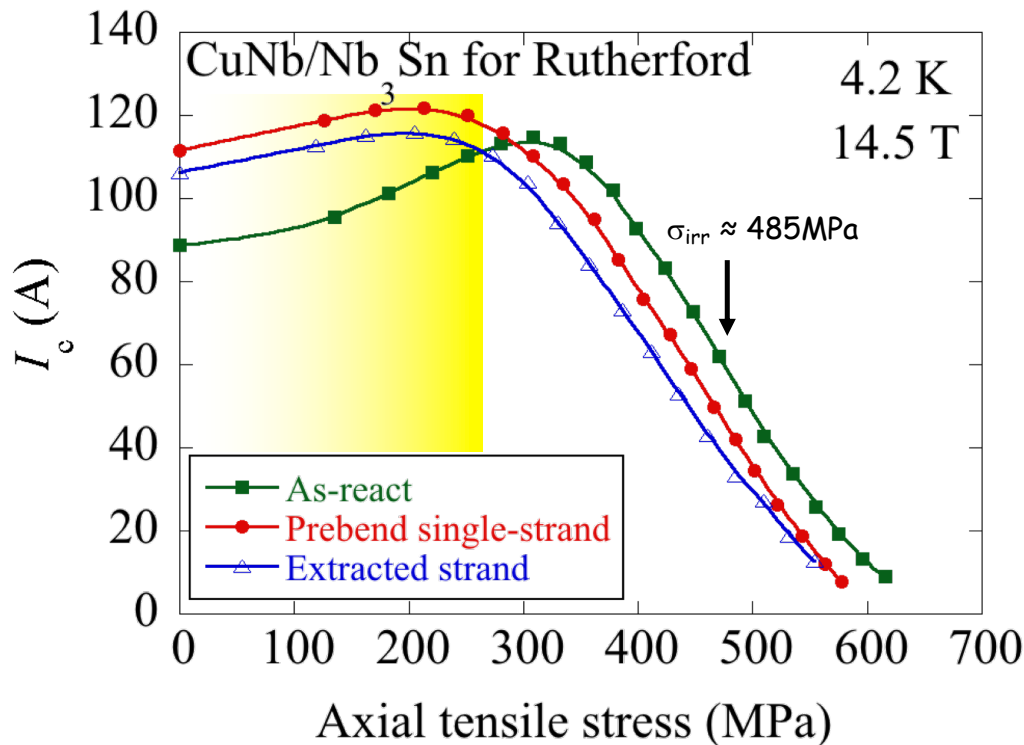
Coil	L1	L2	L3
Inner Dia. (mm)	150	185.9	229.2
Height (mm)	540	628	628
$I_{po}(\text{A})$		854	
B_{max} (T)	13.8 (14.6)*	11.3	8.37
T_{cs} (K)	6.76	8.39	9.95
Trans. stress (MPa)	-38	-49	-48
Hoop stress (MPa)	251 (267)*	243	200

*() w/o energizing the HTS insert



CuNb/Nb₃Sn Rutherford Cable for 25T-CSM

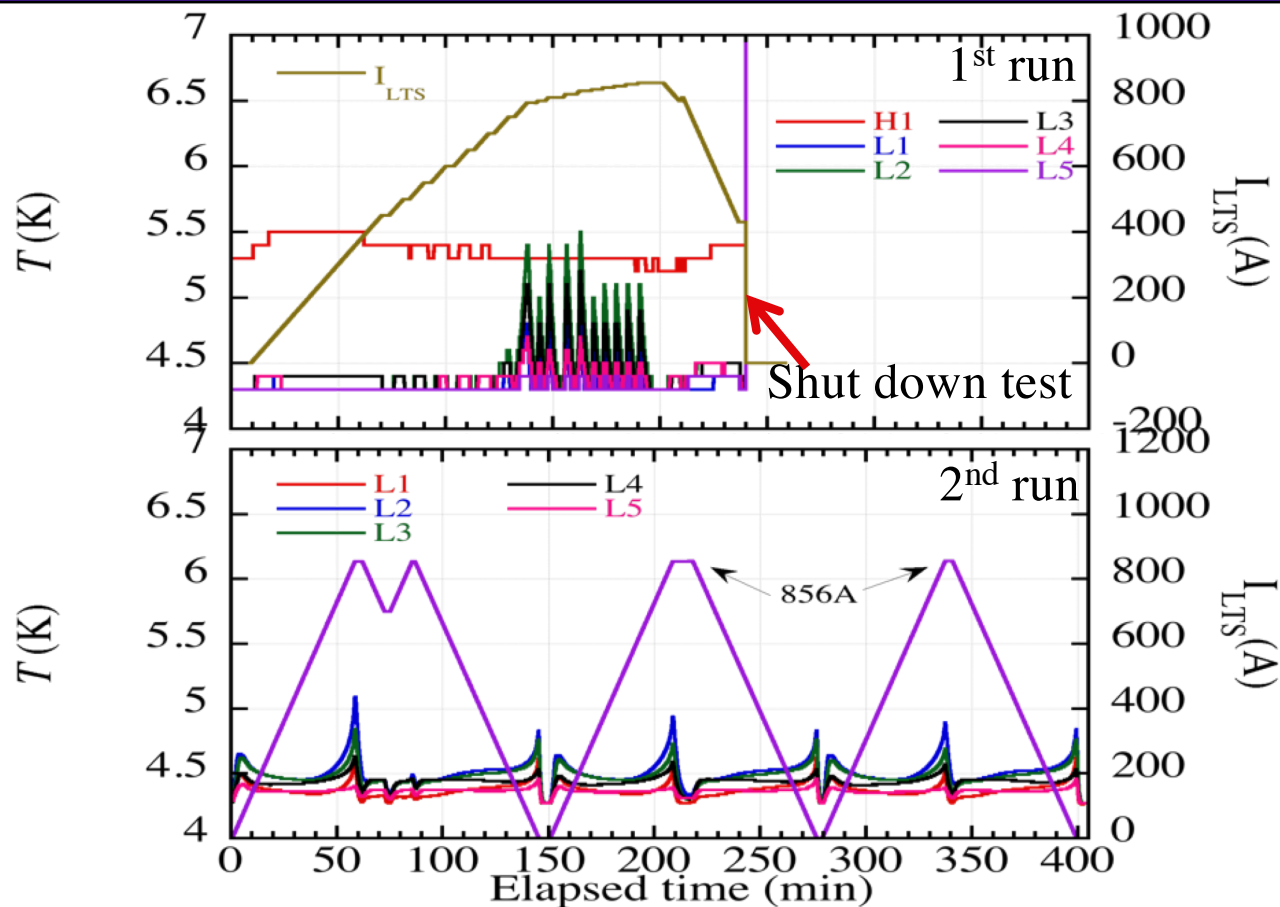
18



- ✓ The Nb₃Sn Rutherford cable optimized by reinforcement and strain control (prebending) is operated in high stress state below 251 MPa (267 MPa in stand-alone operation).



LTS coil for 25T-CSM

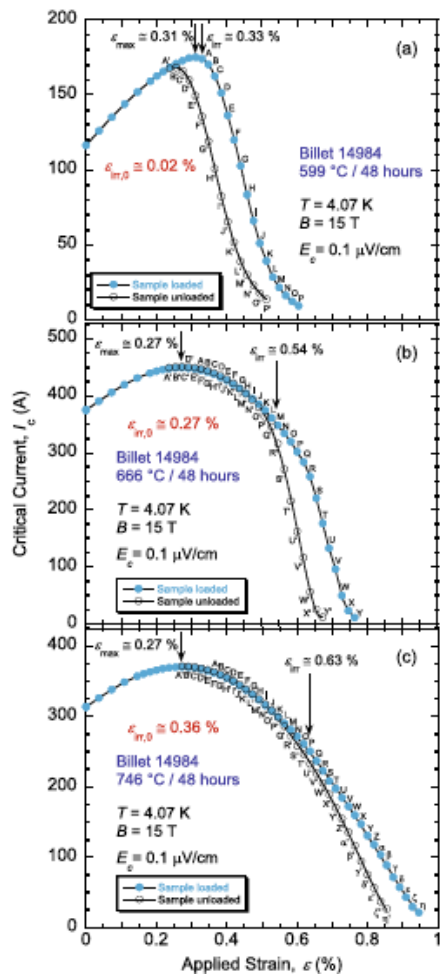


No training quench!

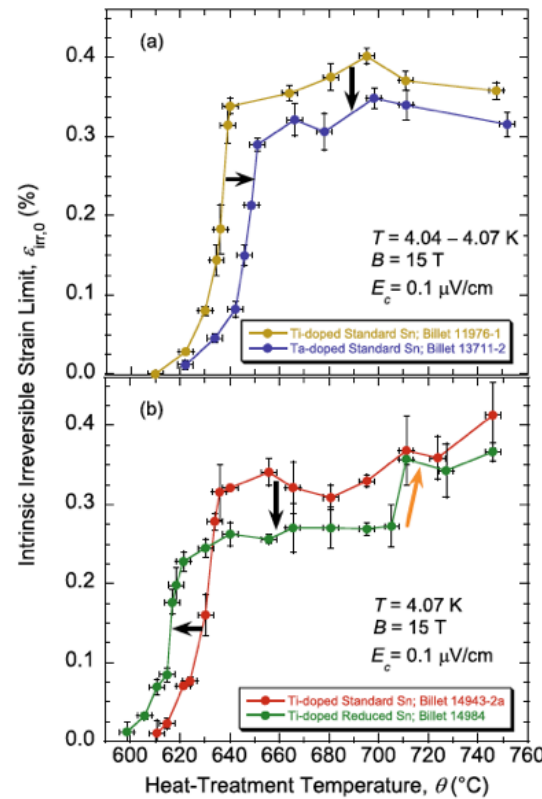
Oguro et al, SuST 29 (2016) 084004



Irreversible strain Cliff in RRP Nb₃Sn wires



N. Chegour et al, Sci. Rep. 9 (2019)9466.



Strain limit (irreversible strain) strongly depends on the HT temperature.



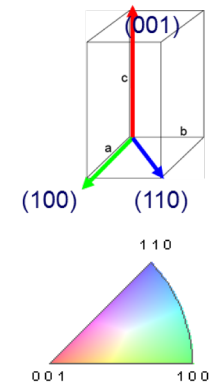
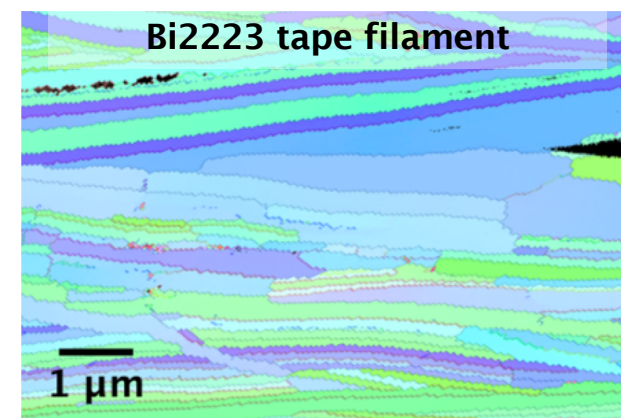
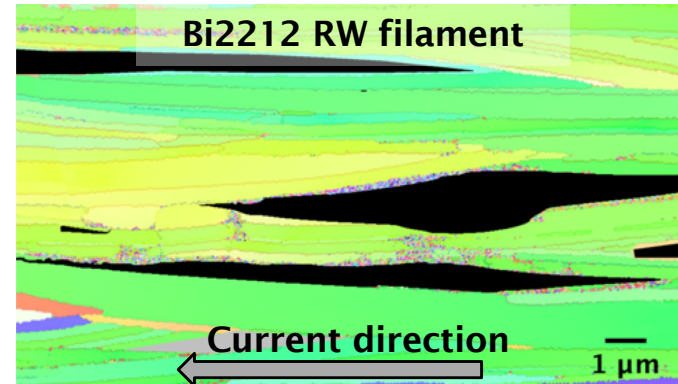
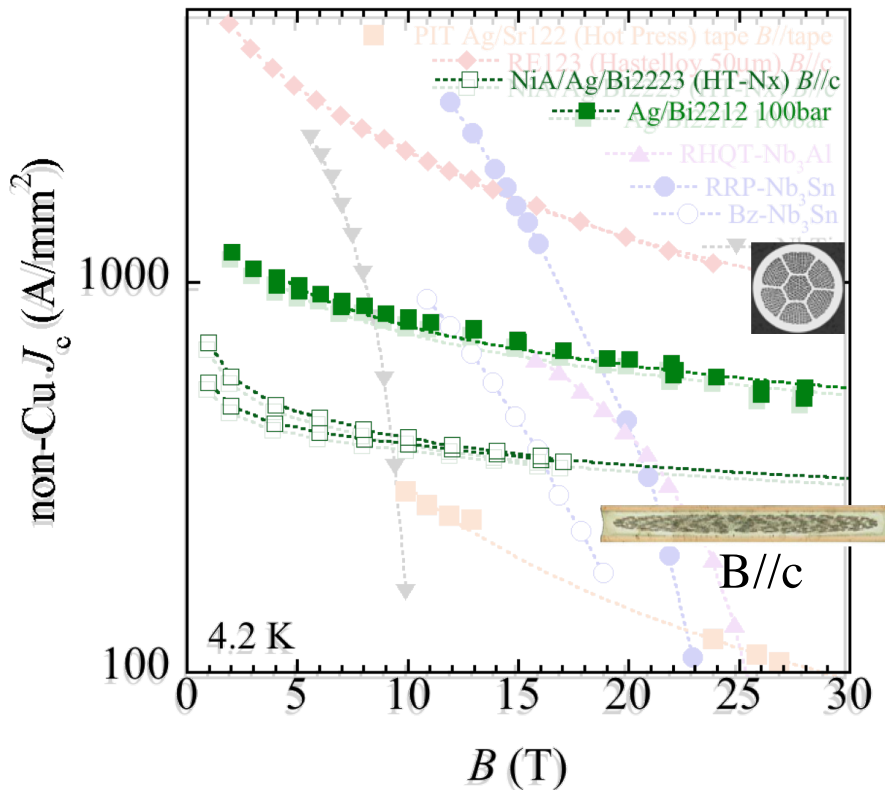
TOHOKU
UNIVERSITY

Bi-Sr-Ca-Cu-O





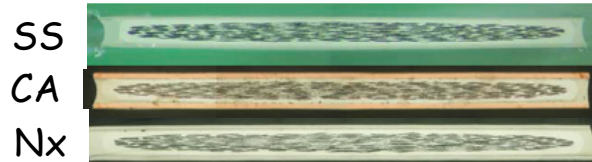
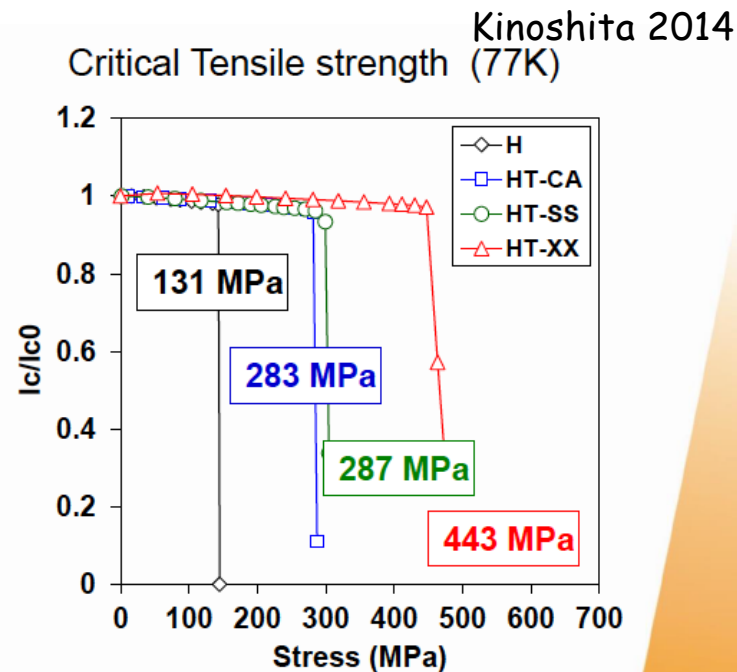
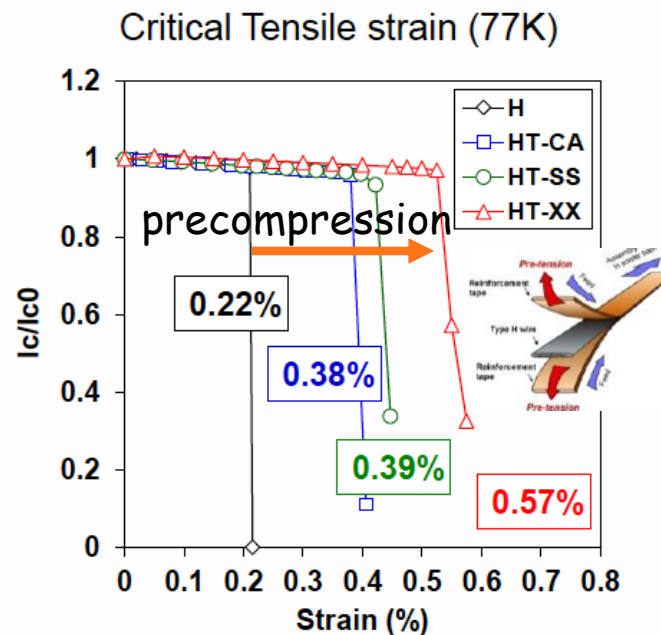
BSCCO



- Both of Bi2212 and Bi2223 have strong c -axis orientation.
- In-plain alignment can be seen only in Bi2212.



High strength Bi2223 tapes by SEI



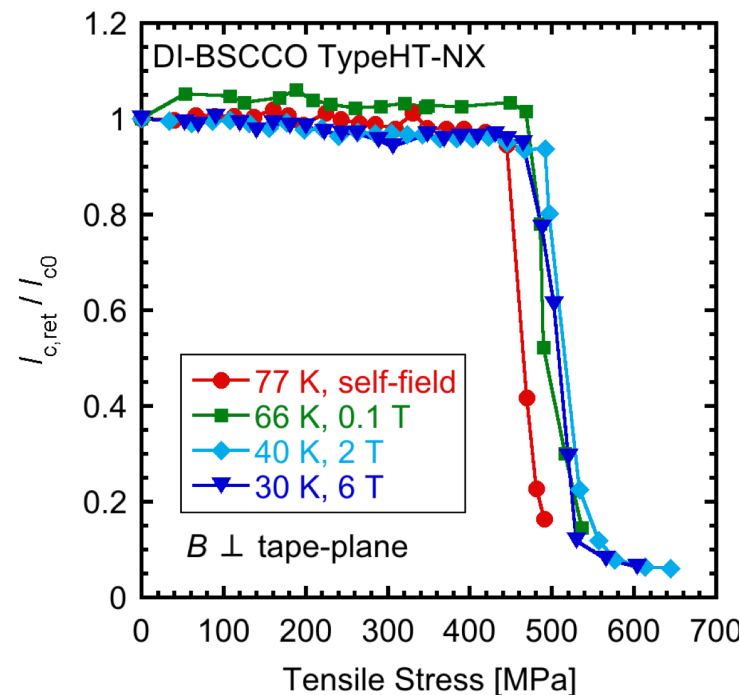
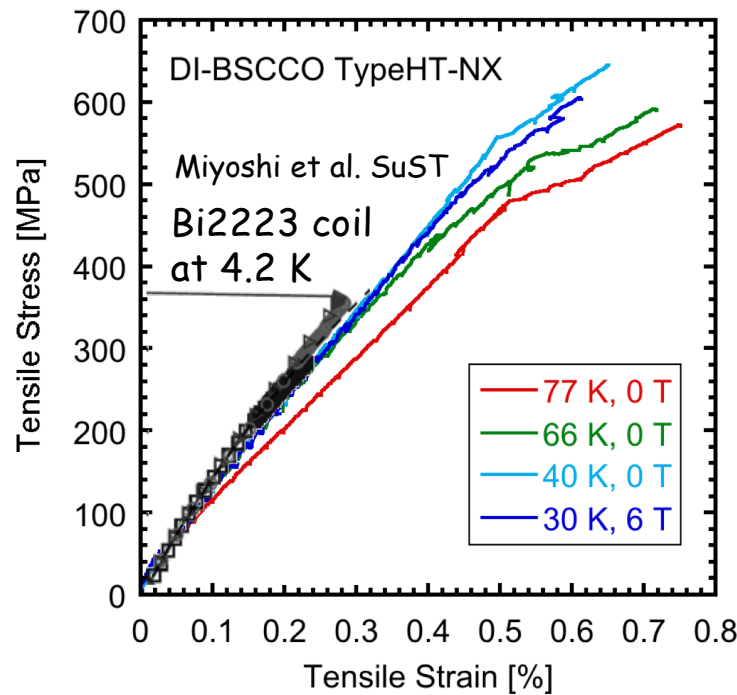
Width: 4.5 mm
 Thickness: 0.28 mm
 I_c : 200A

8

- High strength due to the pre-strain (<0.35%) and reinforcement.
- Improvement of strength is expected with thicker reinforcement.



Mechanical Properties at low temps.



- Stress-strain curves become slightly steeper with temperature decreasing and close to the result of coil at 4K.
- Stress limit more than 400 MPa is not so different with temperature.



Magnet applications with Bi2223

Bi2223 (HT-Nx)

24.6T- 52mm(HFLSM)



$\sigma_{\max} \approx 323 \text{ MPa}$

Open for users since 2016
250 days/year operation

Bi2223 (HT-CA)

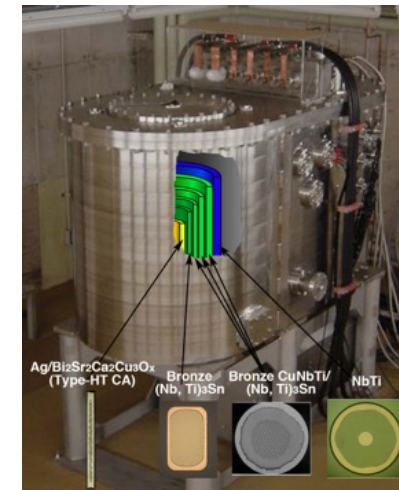
24.2T-53mm (NIMS)
1.02GHz-NMR



$\sigma_{\max} \approx 198 \text{ MPa}$

NMR with 1.02 GHz

20.1T- 52mm(HFLSM)



$\sigma_{\max} \approx 118 \text{ MPa}$

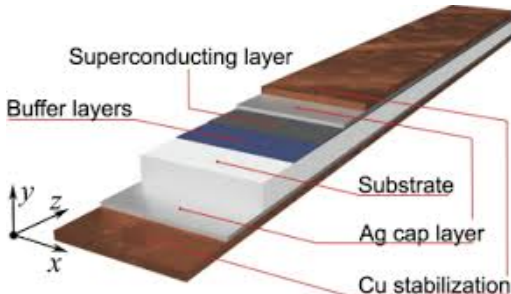
Open for users since 2013
>250 days/year operation



TOHOKU
UNIVERSITY



Commercial REBCO tapes



Fujikura

SuperPower
A Fujikawa Company

SuNAM

SUPEROX JAPAN
SUPERCONDUCTIVITY FOR LIFE

上海超导
SHANGHAI SUPERCONDUCTOR

Bruker EST
A Bruker Company

American Superconductor®

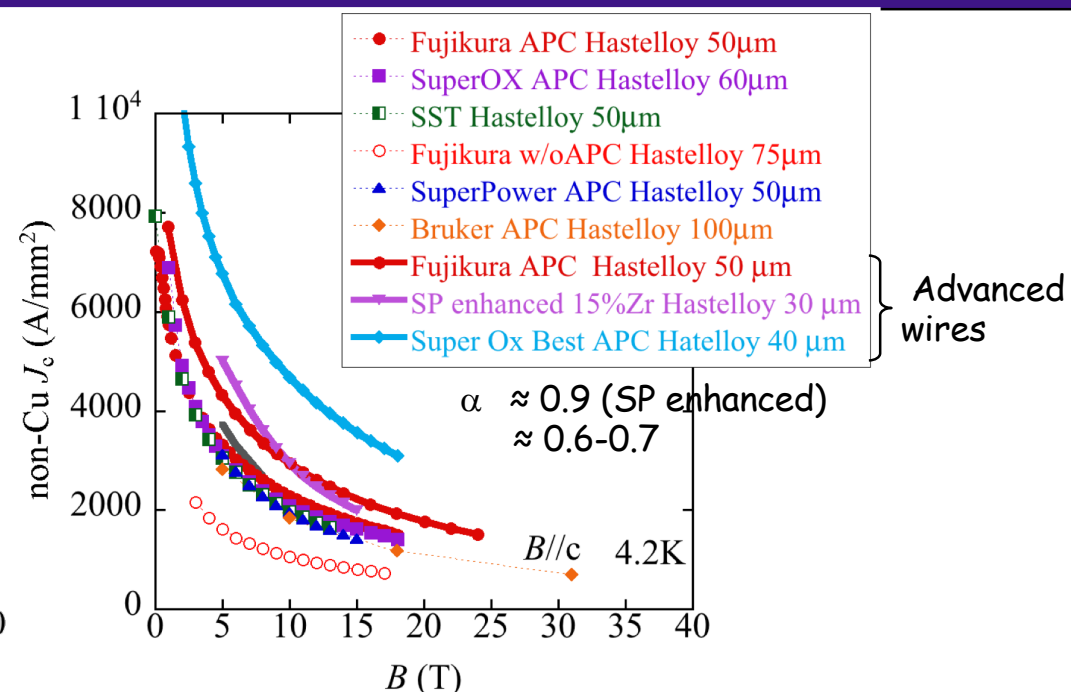
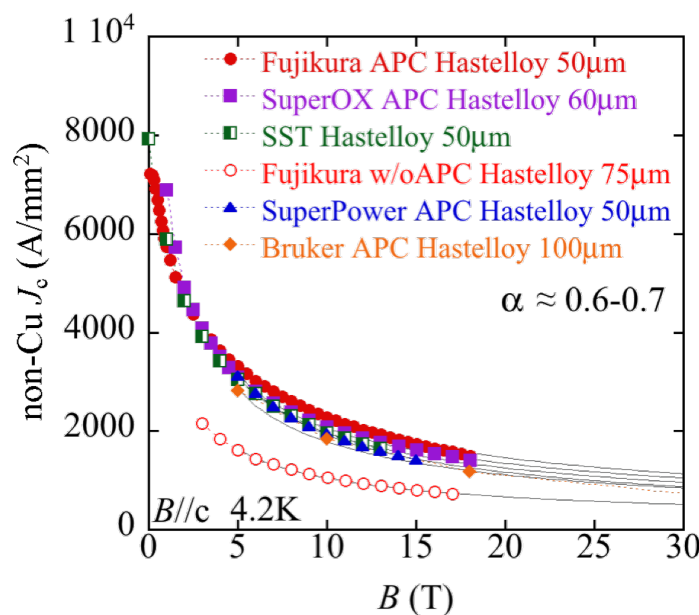
THEVA

STI
SUMITOMO ELECTRIC
Connect with Innovation

	RE	Method	t_SC (um)	APC	Template	Sub	t_sub (um)	Stabilizer	t_stab (um)
Fujikura	Gd	PLD	≈2	-	IBAD-MgO	Hastelloy	75	Cu plated	10-40 × 2
	Eu		≈2.5	Hf			50		
SuperPower	Y,Gd	CVD	≈1.5	Zr	IBAD-MgO	Hastelloy	(30), 50	Cu plated	20,40 × 2
SuNAM	Gd	RCE	1.3-1.8	-	IBAD-MgO	Hastelloy /SS	60	Cu plated	5-10 × 2
SuperOx	Gd	PLD	2.3-2.5	-	IBAD-MgO	Hastelloy	40, 60	Cu plated	1-50 × 2
	RE		2.3-2.7	Hf					
SST	RE	PLD	≈2.4	Not Open	IBAD-MgO	Hastelloy	30,50	Cu plated	5-10 × 2
Bruker	Y	PLD	1.5-1.7	Nano Rod	ABAD-YSZ	SS	100	Cu plated	40 × 2
AMSC	Y,Dy	MOD	0.8-1.2	Dy ₂ O ₃	RABiTS	NiW	≈100	Cu, Brass, SS laminated	50 × 2
THEVA	Gd	PVD (EB)	≈2.5	-	ISD-MgO	Hastelloy	50, 100	Cu PVD / laminated	30, 40, 100 (lamination) <20 × 2 (PVC)
STI	Y	RCE-CDR		-	IBAD-MgO	Hastelloy	100	Cu PVD	20 × 2
SEI	Gd	PLD		-	Textured-Cu	SS	100	Cu plated	20 × 2

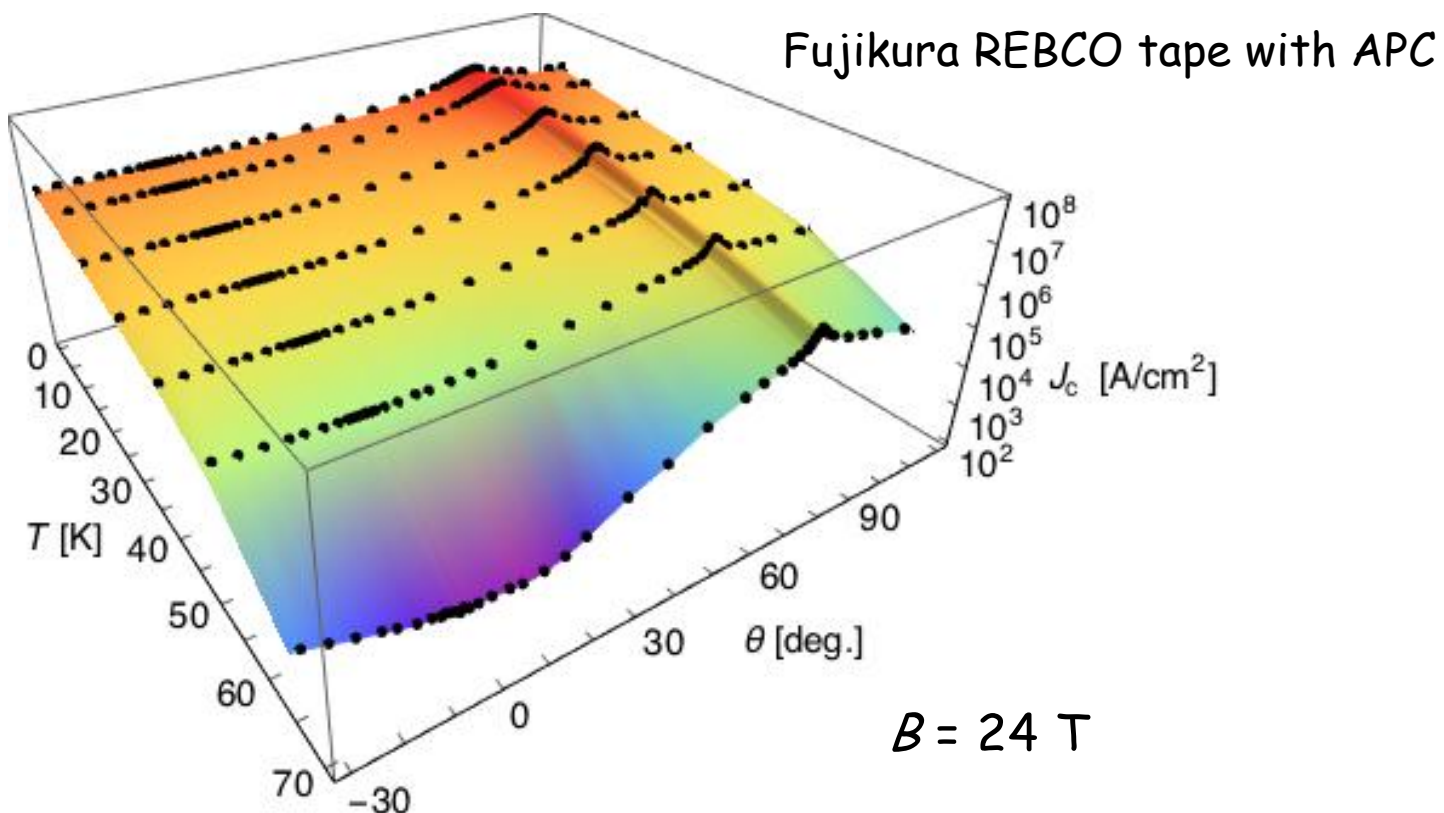


Non-Cu J_c of REBCO commercial tapes



- APC is effective even in low temperatures and high fields.
- Many vendors introduce APC.
- Non-Cu J_c increases with a reduction of substrate thickness and an increase of REBCO thickness.
- Increase REBCO thickness is effective to increase non-Cu J_c but may increase cost and delamination risk.

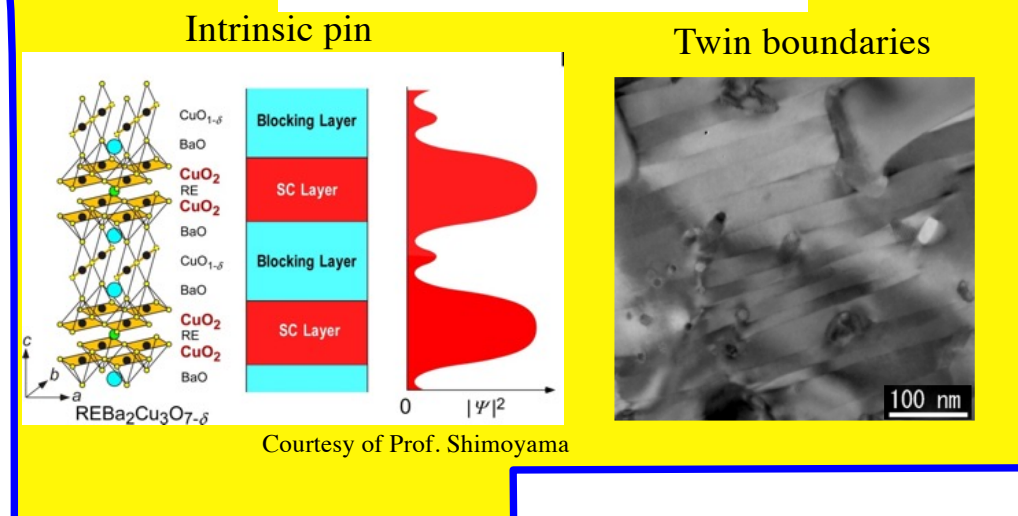
Typical angular dependence of J_c for REBCO tapes



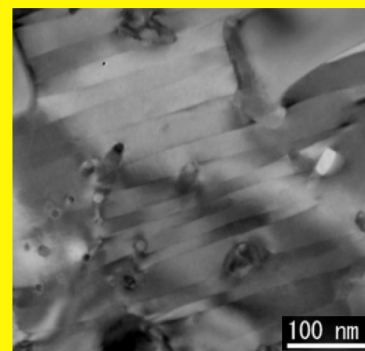


Flux pinning centers in REBCO

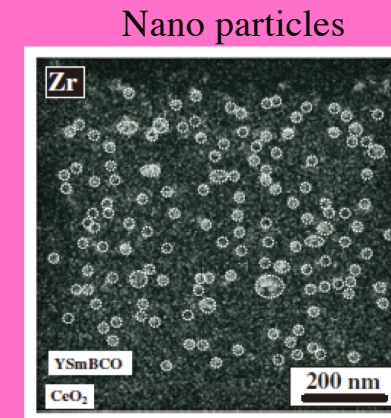
Natural pinning centers



Twin boundaries

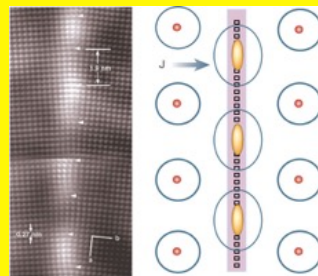


Artificial pinning centers



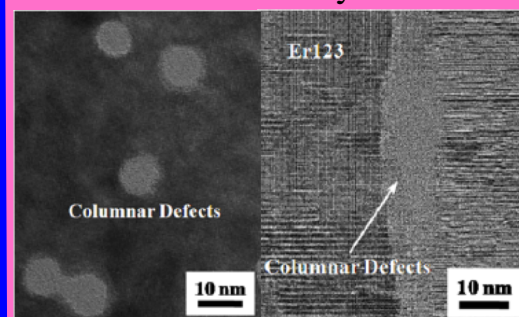
Miura et al., APEX 2009

Edge dislocations at GB

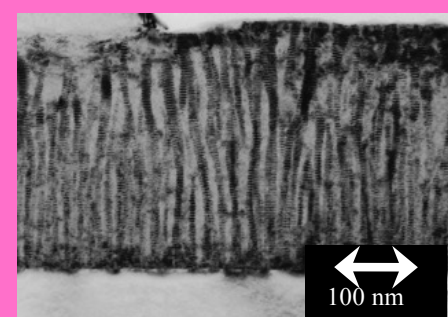


D. Larbalestier, Nature 414(2001)368

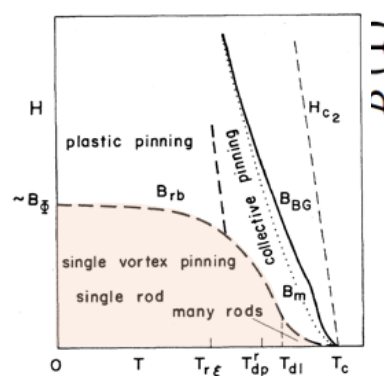
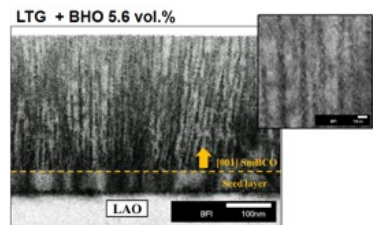
Columnar defects by irradiation



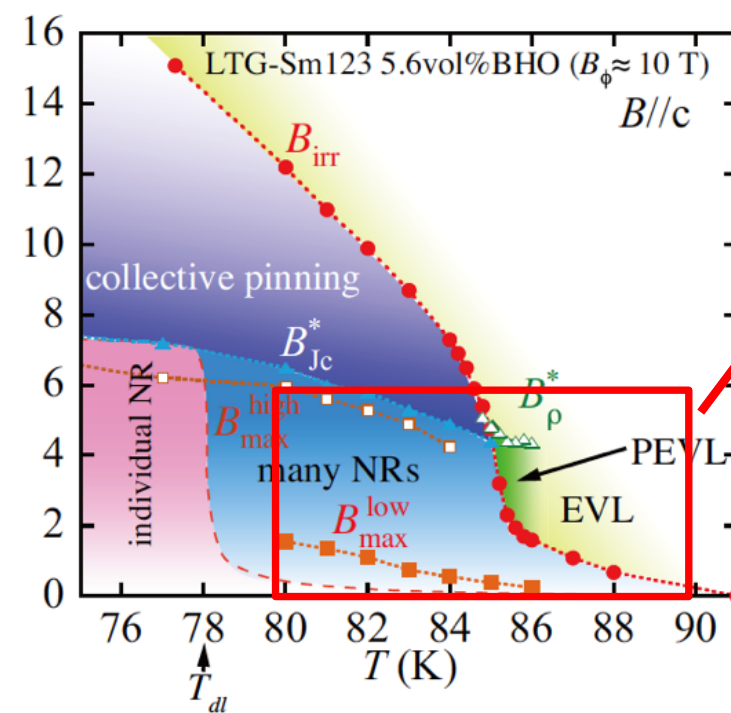
Nano rods



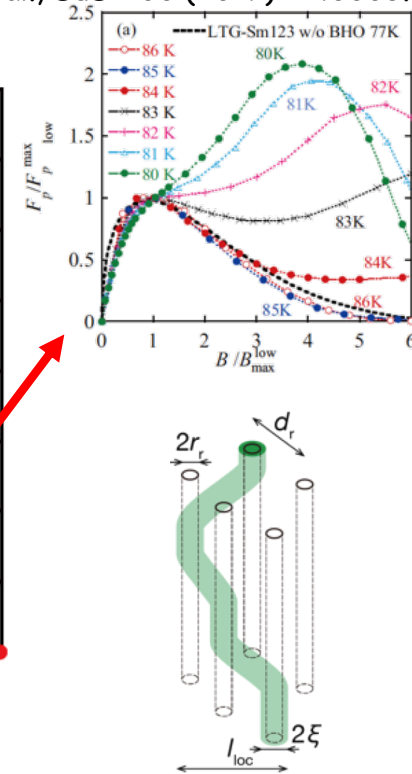
Flux pinning phase diagram (High Temperature)



G. Blatter et al., Rev. Mod. Phys. **66**, 1125 (1994).



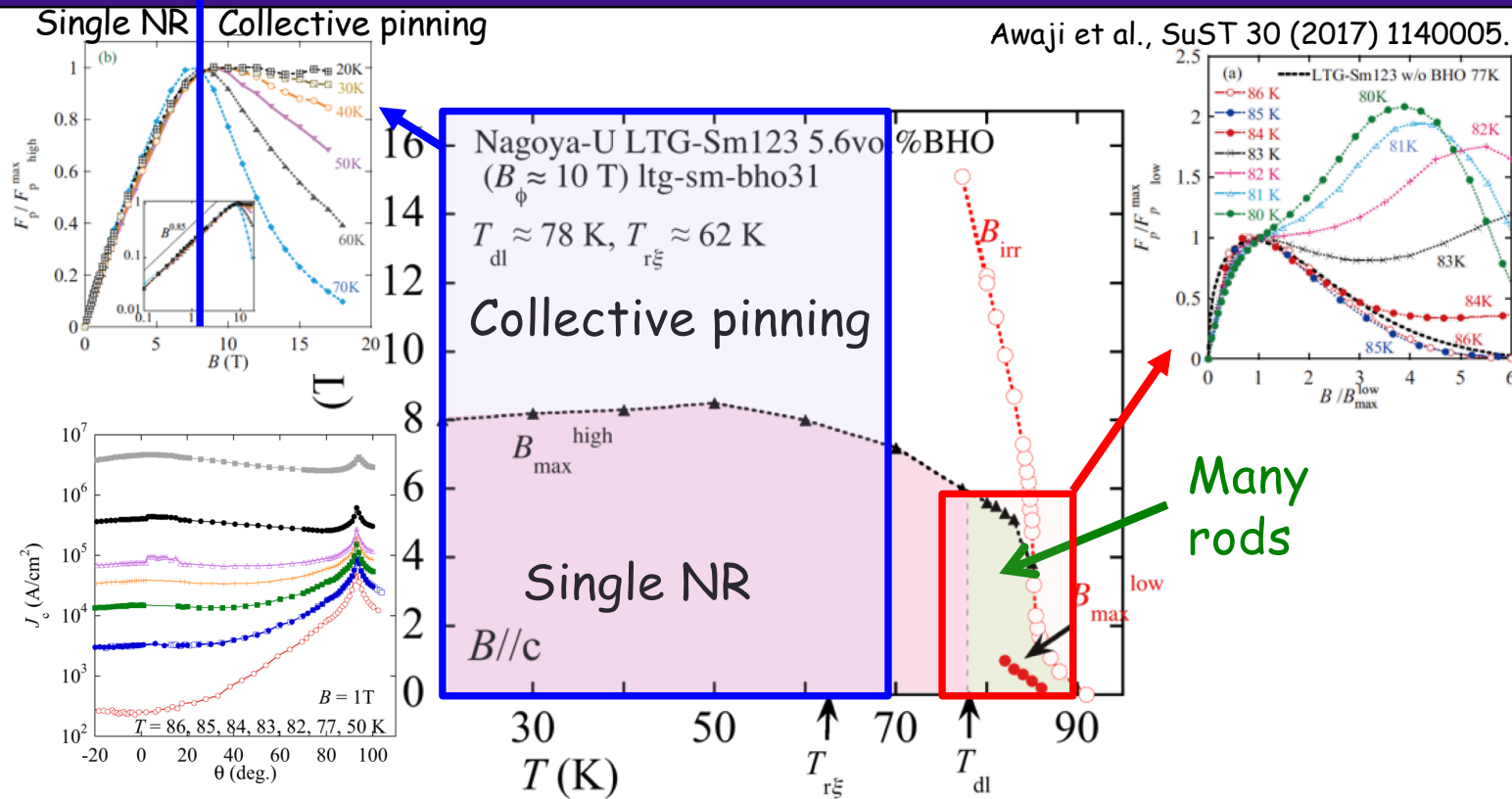
Awaji et al., SuST 30 (2017) 1140005.



The correlated pinning strength in many NRs shrinking rapidly with increasing T toward to T_{dl} . The random and correlated pins competed in HT. The correlated pinning becomes dominant below T_{dl} and B_ϕ .



Flux pinning phase diagram

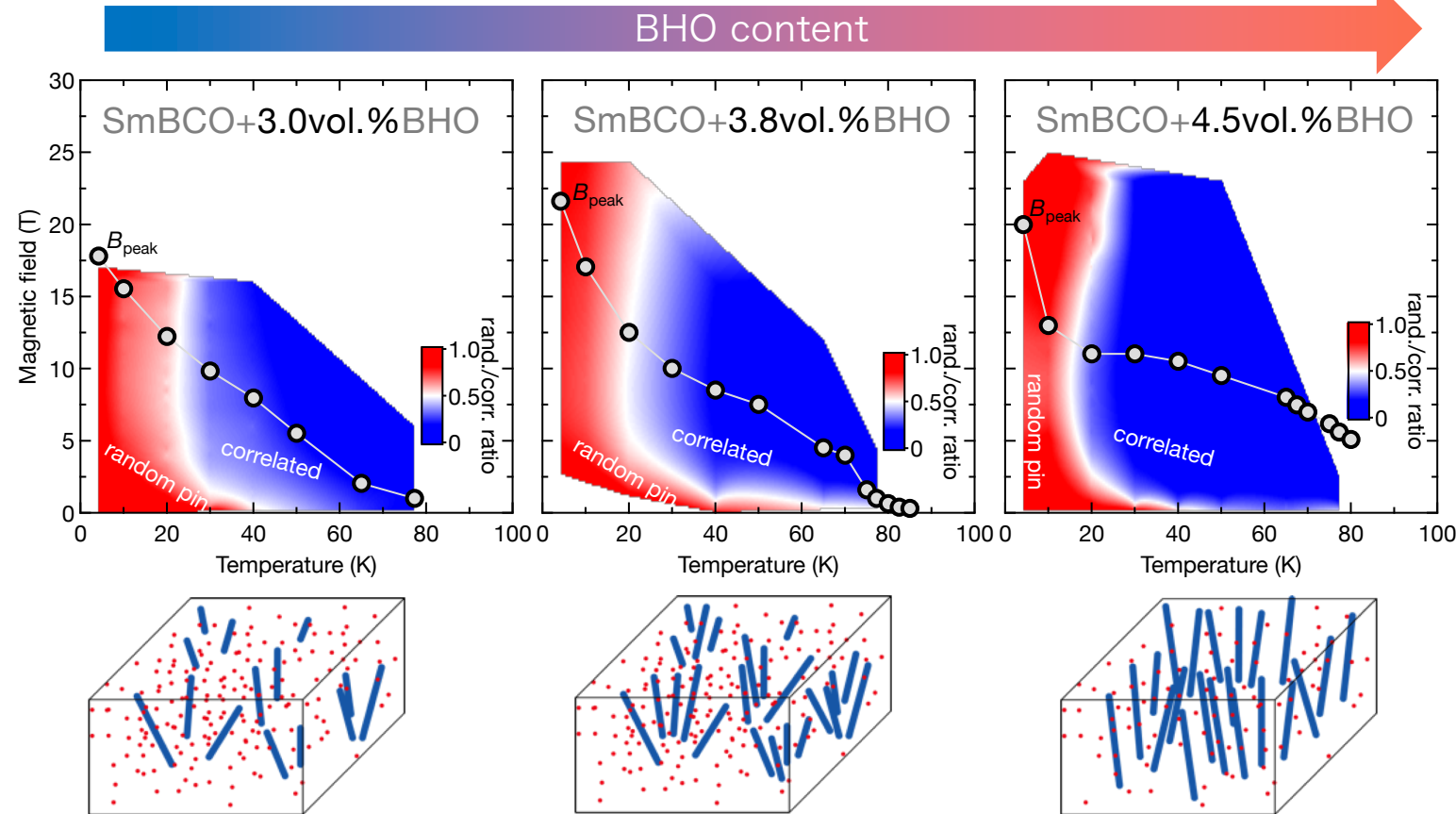


The correlated pinning strength in many NRs increases rapidly with T -decreasing toward to T_{dl} . The random and correlated pins competed in HT. The correlated pinning becomes dominant below T_{dl} and B_ϕ .



Inclined nanorods

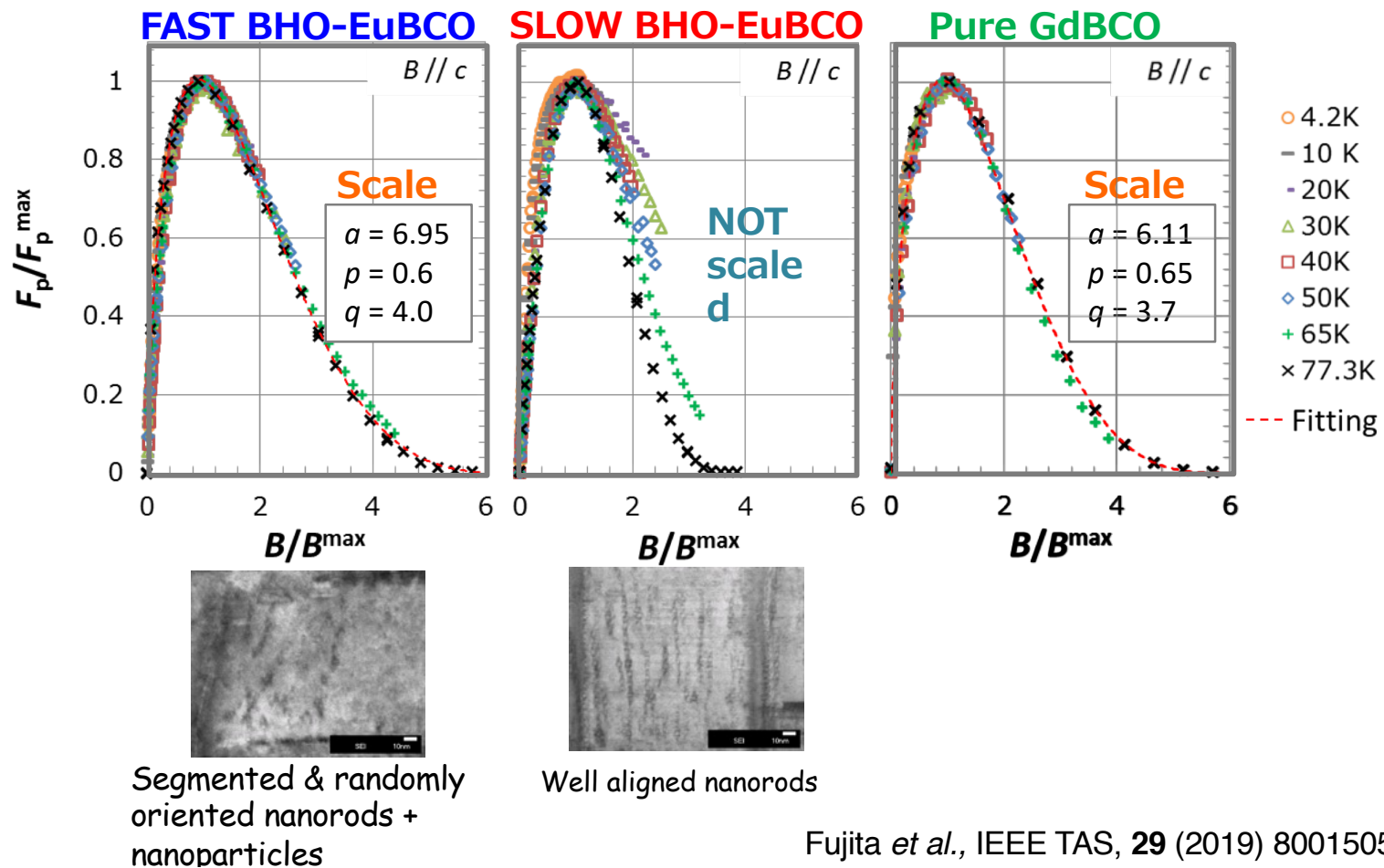
Tsuchiya et al., SuST 30 (2017) 104004





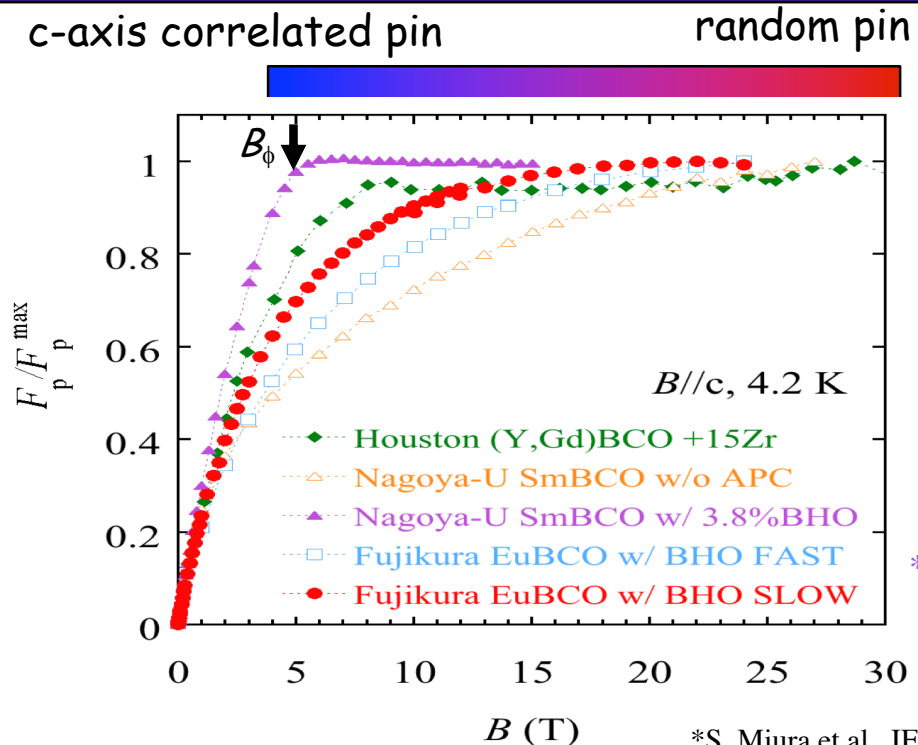
Flux pinning force density, F_p

34





Comparison of F_p/F_p^{\max} curves at 4.2K



*S. Miura et al., IEEE TAS 28 (2018) 8000606.

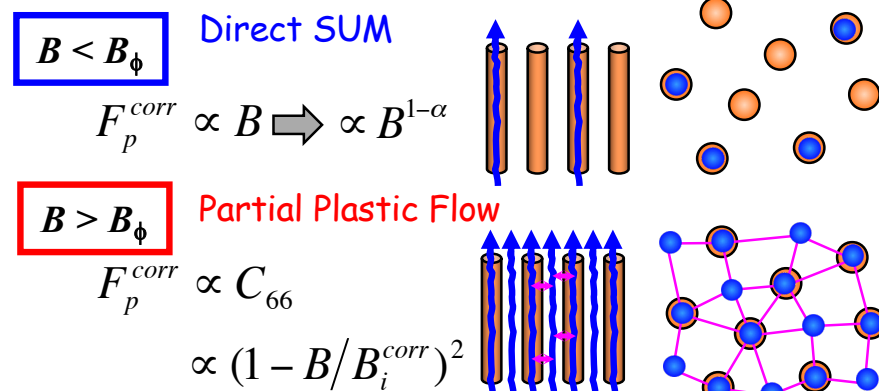
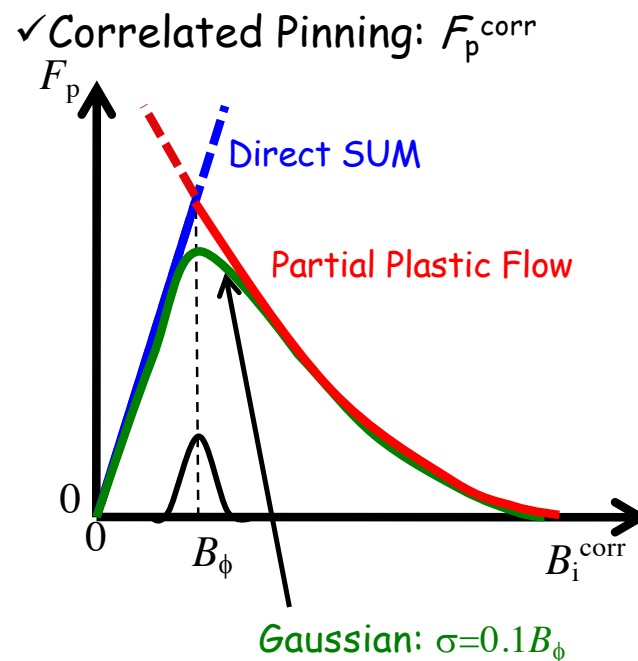
- ✓ B_{\max} becomes higher with stronger random pinning.
- ✓ Fluctuation of growth direction and segmentation of nanorod enhances random pinning behavior.
- ✓ Practical REBCO tapes are in the intermediate state between random and correlated pinning states.

Cooperative pinning model - correlated pinning -

$$F_p = \sqrt{(F_p^{\text{rand}})^2 + (F_p^{\text{corr}})^2} : B > B_\phi$$

$$F_p = F_p^{\text{corr}} : B < B_\phi$$

F_p^{rand} : Random pinning force density
 F_p^{corr} : Correlated pinning force density



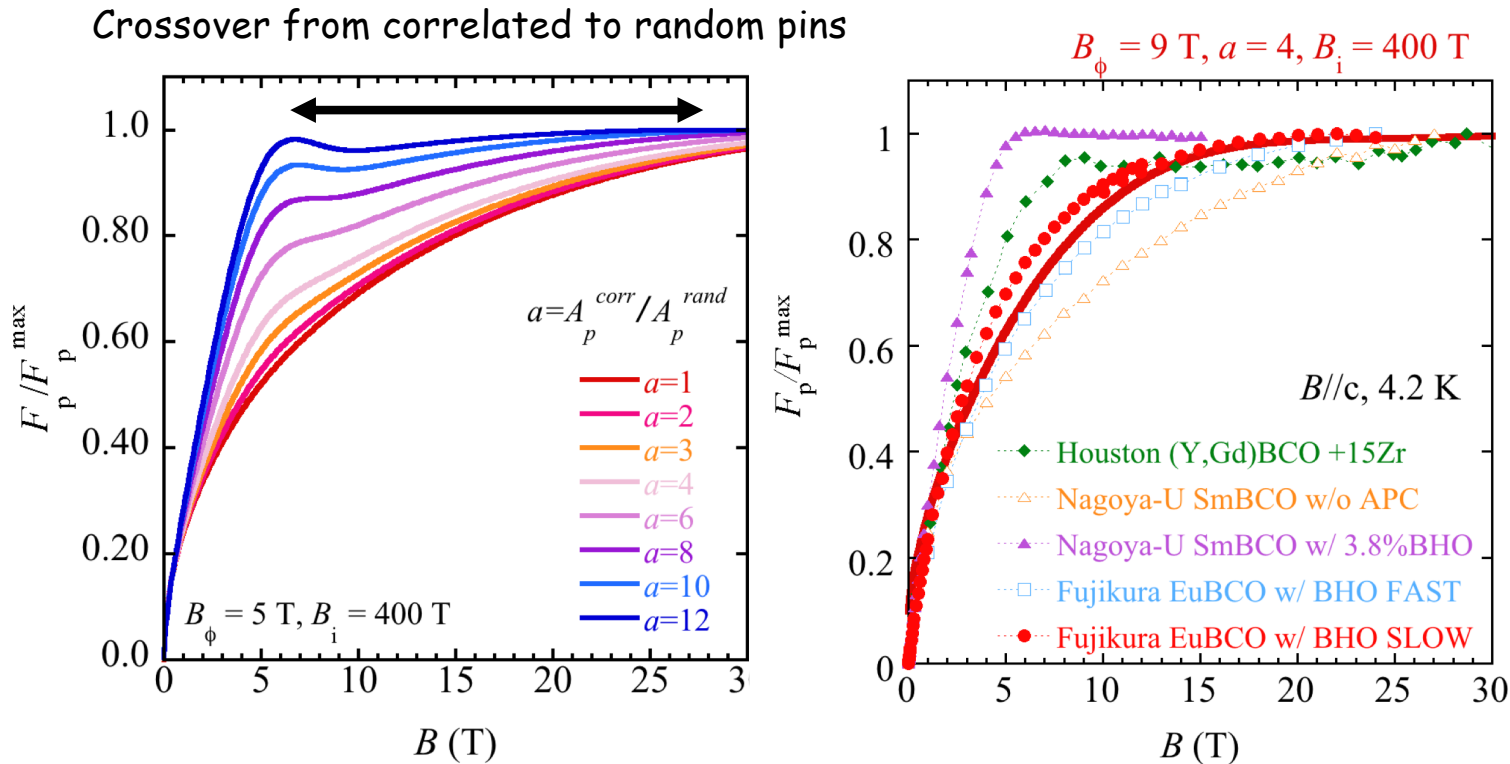
α : magnetic field sensitivity parameter for the nanorod.
 $(\alpha=0$ for the ideal c-axis correlated pin $)$

$$F_p^{\text{corr}} = \begin{cases} A_{\text{corr}} b_{\text{corr}}^{1-\alpha}, & b \leq b_\phi \\ \frac{A_{\text{corr}} b_\phi}{(1-b_\phi)^2} (1-b_{\text{corr}})^2, & b > b_\phi \end{cases}$$

S. Awaji *et al.*, IEEE TAS **21** (2012) 3192
S. Awaji *et al.*, JAP **111** (2012) 013914.



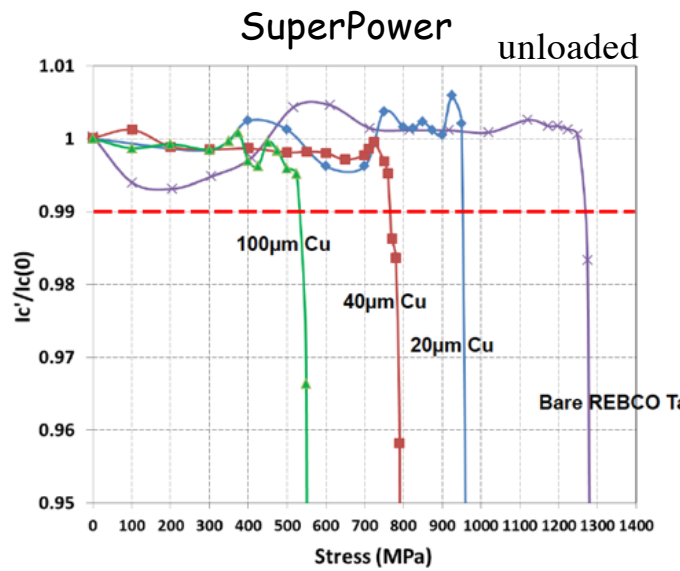
Calculation results



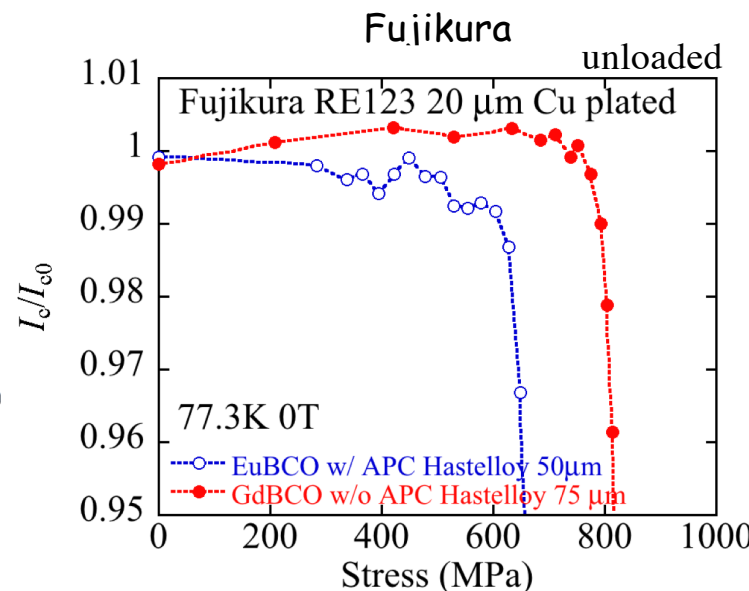
- ✓ Stronger random pinning contribution shifts F_p peak to higher field.



Electromechanical properties in REBCO



Y. Zhang et al., IEEE TAS 26 (2016) 8400406.

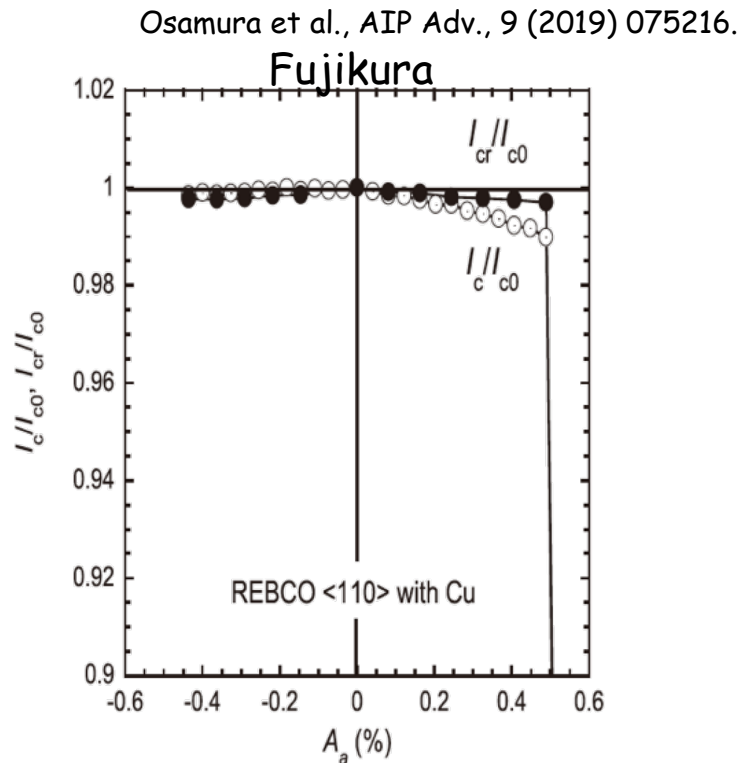
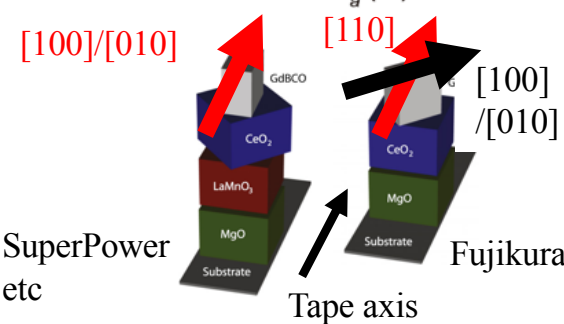
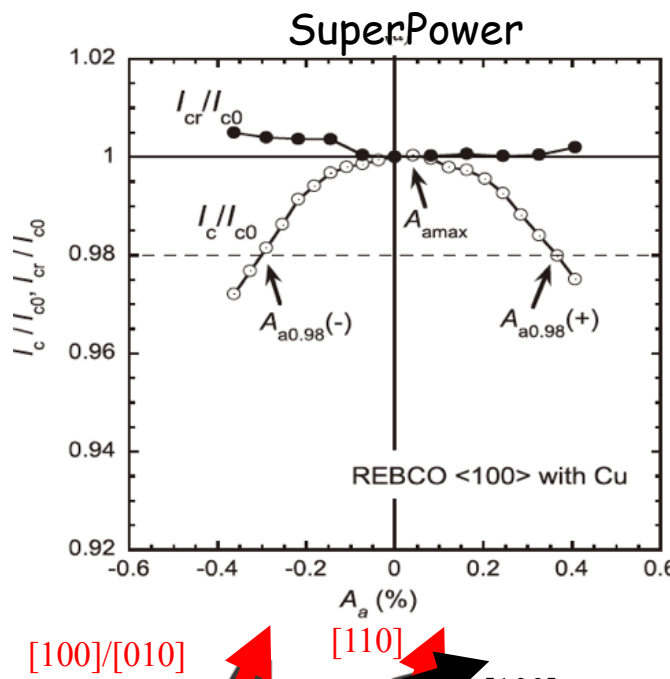


S. Fujita et al., IEEE TAS 24 (2015) 840304.

- ✓ Stress tolerances decreases with increasing Cu and decreasing Hastelloy.
- ✓ Hastelloy thickness tends to decrease for increase J_e recently.



Strain dependence of J_c in REBCO tapes

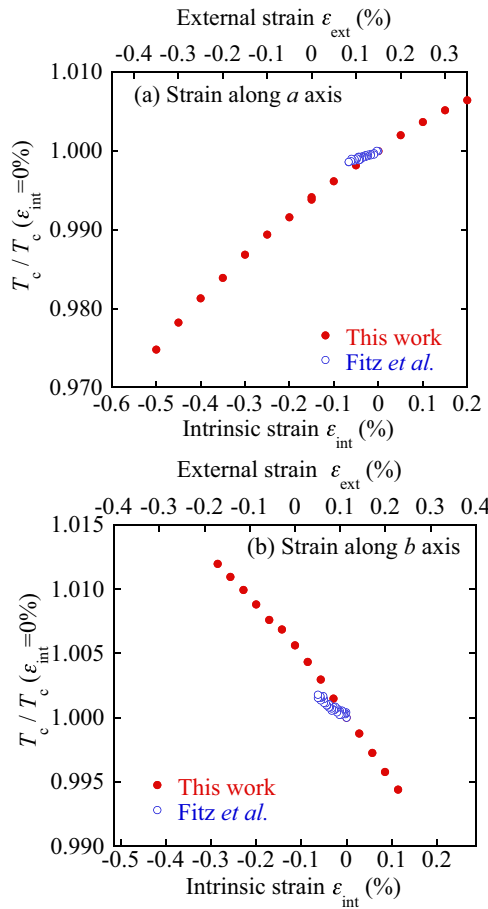


Strain dependence is more sensitive along [100]/[010] than along [110].

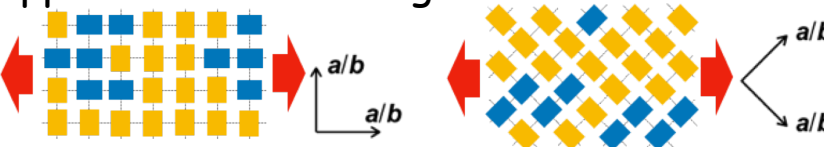


Strain dependence of T_c along a - and b - axes

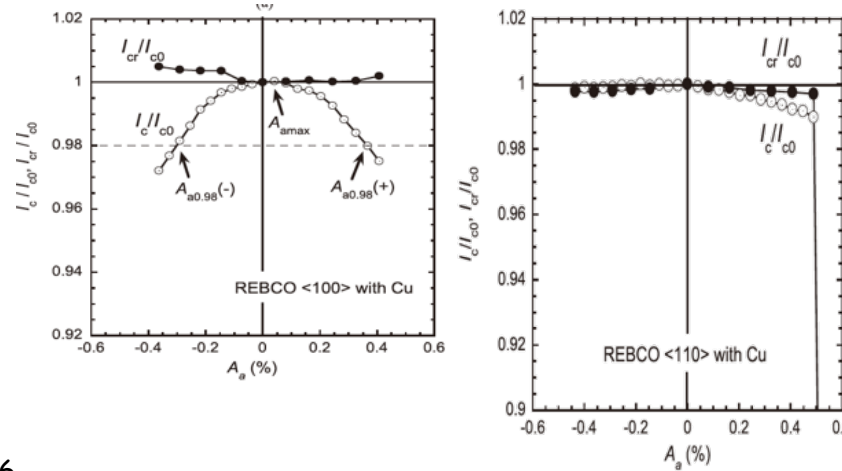
40



- Strain dependence along a - axis is opposite to that along b -axis.



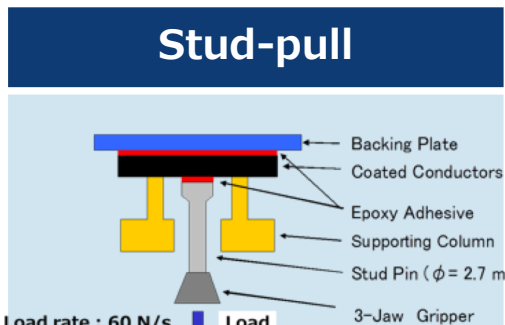
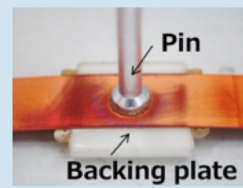
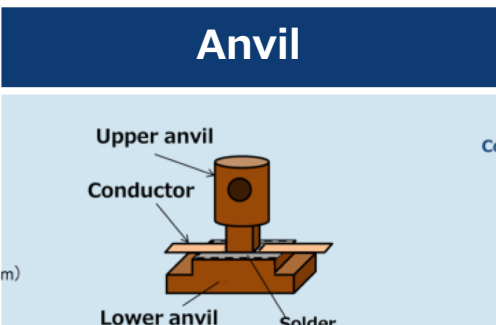
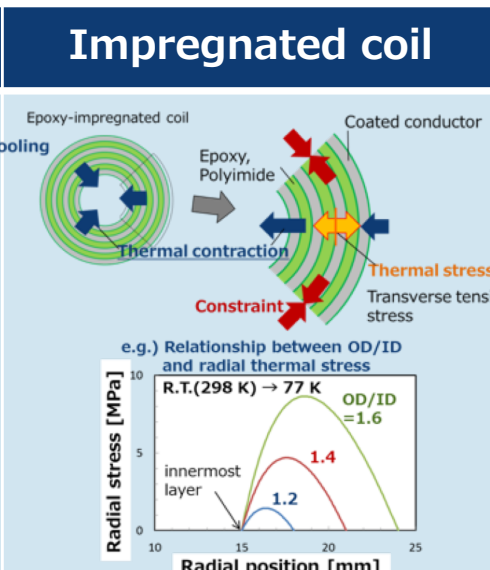
- Strain along [110] cancels the strain dependences along [100] and [010] which are opposite each other.



S. Awaji et al., Sci. Rep. 5 (2015) 11156.



Delamination in REBCO tapes

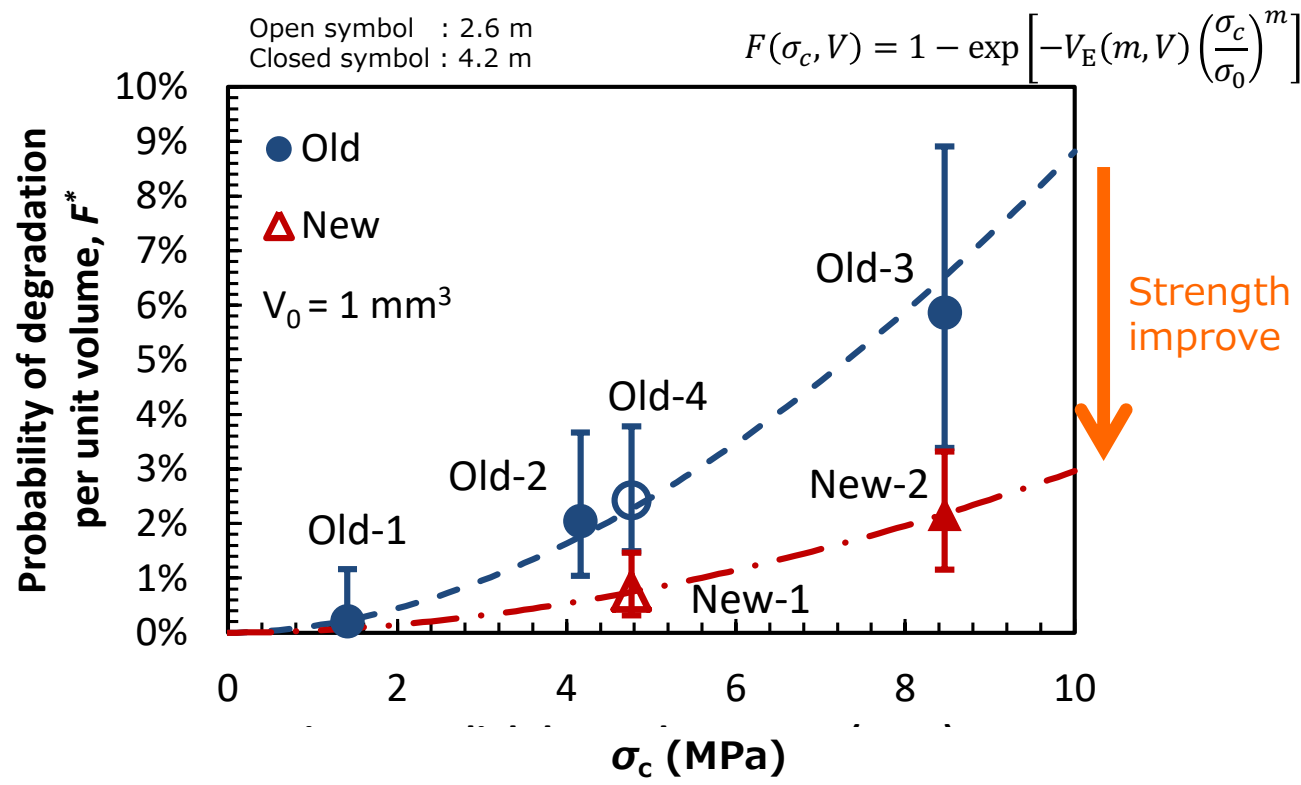
Stud-pull	Anvil	Impregnated coil
  <p>Test area : 5.7 mm² $(\phi 2.7 \text{ mm pin})$ Strength : ~ 40 MPa</p> <p>T. Oyama, et al., Journal of The Surface Finishing Society of Japan, 58 (2007) P. 292</p>	  <p>Test area : 32 mm² $(4 \times 8 \text{ mm anvil})$ Strength : ~ 10 MPa</p> <p>H. Shin, et.al., SuST, 27 (2014) 025001</p>	 <p>Test area : 16000 mm² $(4 \text{ mm}^w \times 4 \text{ m coil})$ Strength : ~ 5 MPa</p> <p>H. Miyazaki et al., IEEE TAS, 25 (2015) 6602305</p>

Delamination strength depends on the methods



Courtesy of S. Muto (Fujikura)

Weibull analysis considering size effect



- Delamination strength as a function of volume-> depending on thickness
- Is Local degradation unavoidable?
-> Need strategy for the local degradation in REBCO magnet.



TOHOKU
UNIVERSITY

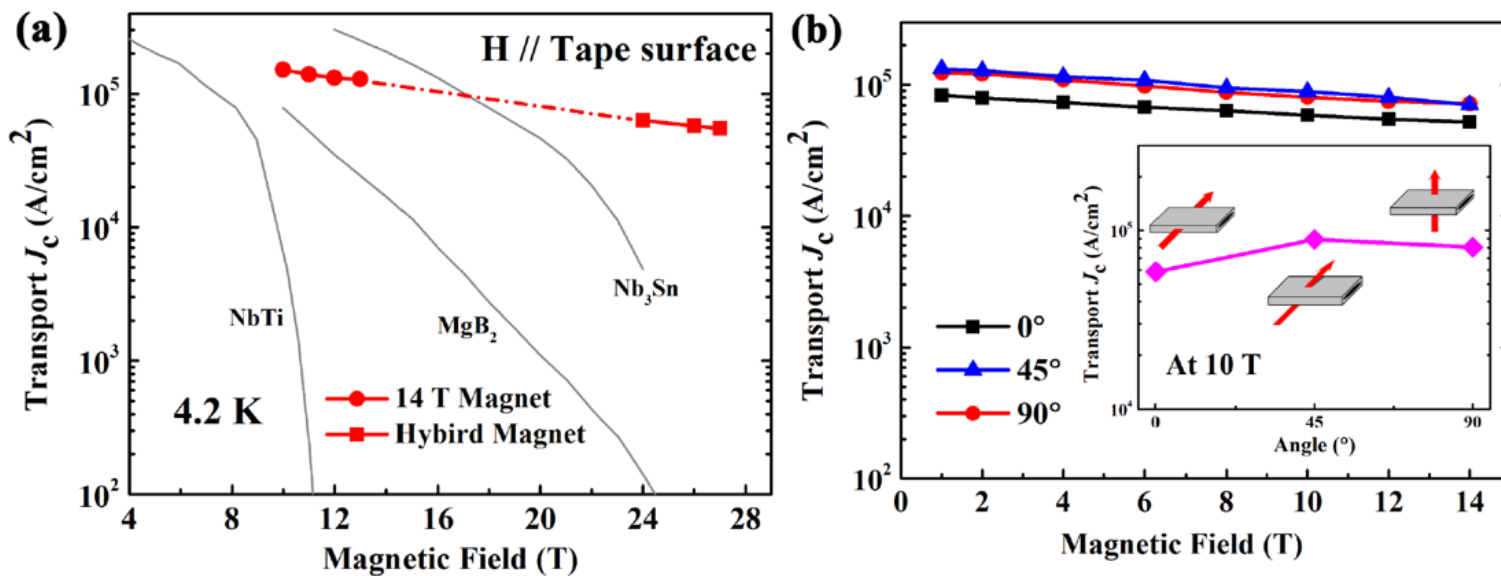
Fe-based Superconductor $(\text{Ba}, \text{K})\text{Fe}_2\text{As}_2$



Courtesy of Prof. Ma

High transport J_c values were achieved in Ba122/Ag tapes

At 4.2K, 10 T, $I_c=437$ A, $J_c\sim150000$ A/cm²



At 4.2K, 14 T, $J_c\sim140000$ A/cm²

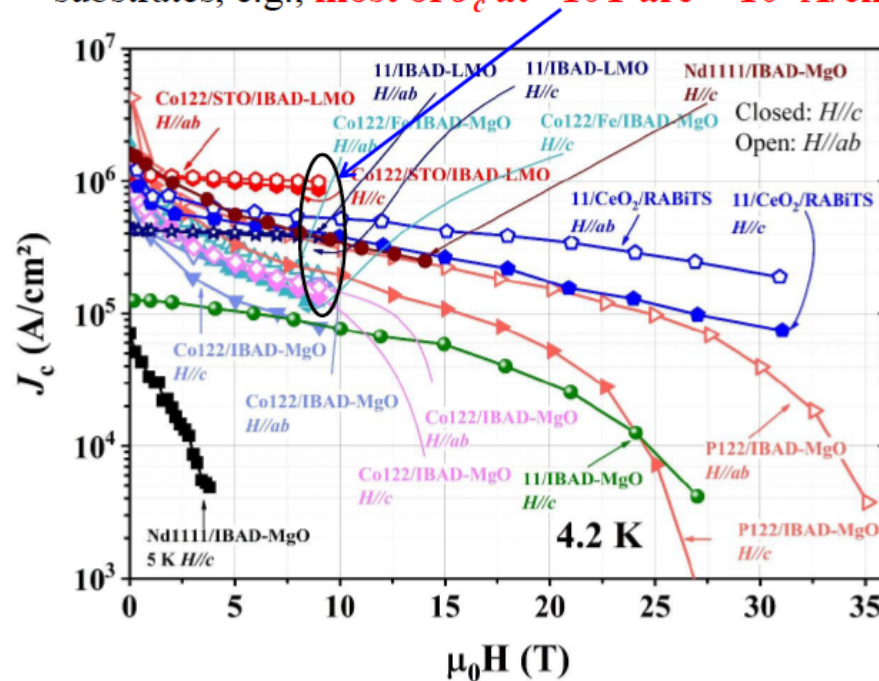
At 4.2K, 27 T, $J_c\sim55000$ A/cm²

The anisotropy of
 J_c at 10T is 1.37

H. Huang, et al., *SuST* 31 (2018) 015017

Sumary: J_c of different IBS coated conductors

- ◆ From the point of view of possible applications, many groups tried film deposition on technical substrates.
 - ◆ Three main systems (11, 122, and 1111) with superior J_c have already been realized on technical substrates, e.g., **most of J_c at ~10T are $> 10^5$ A/cm², from 10^5 to 10^6 A/cm²**.



The J_c anisotropy of 11 and 122 was quite small

To further improve J_c , the introduction of APC is necessary.

K. Iida *et al.* APL 105, 172602 (2014)

Courtesy of K. Iida

S. Trommler *et al.* *SuST* 25, 084019(2012)

T. Katase *et al.* APL 98, 242510 (2011)

H. Hiramatsu et al. SuST 30, 044003(2017)

K. Iida et al. Sci. Rep. 7, 3995 (2017)

Z. T. Xu *et al.* *SuST* 31, 055001 (2018)

W. S. C. Chang et al. / *SUST* 30, 035003 (2017)

W. Si et al. *Nat. Commun.* 4, 1347 (2013)

W. Si *et al.* APL 98, 262509 (2011)

Task: to develop simpler and scalable techniques for making long coated conductors

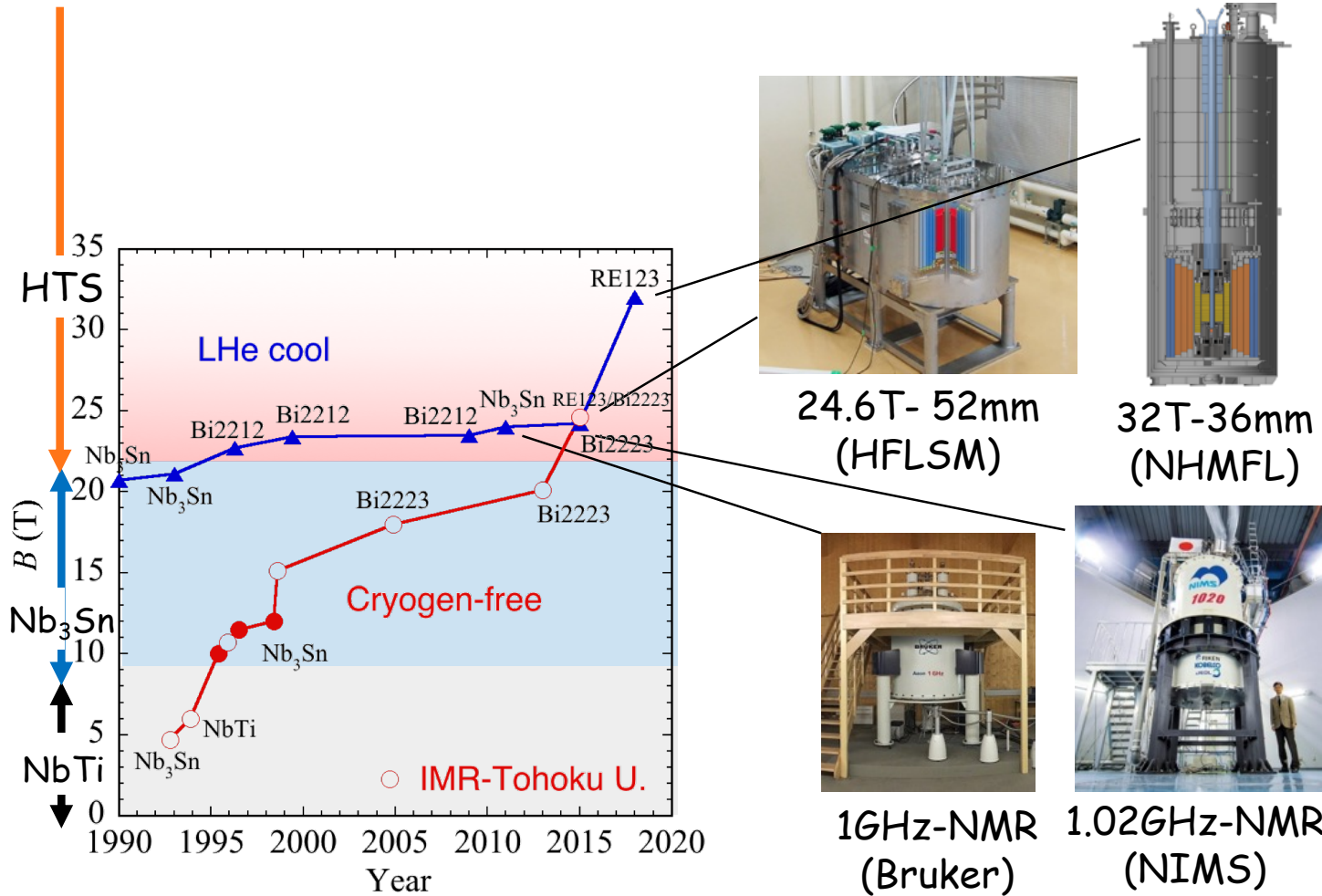


TOHOKU
UNIVERSITY

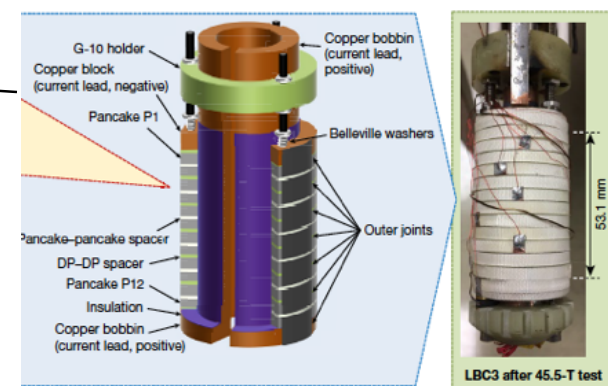
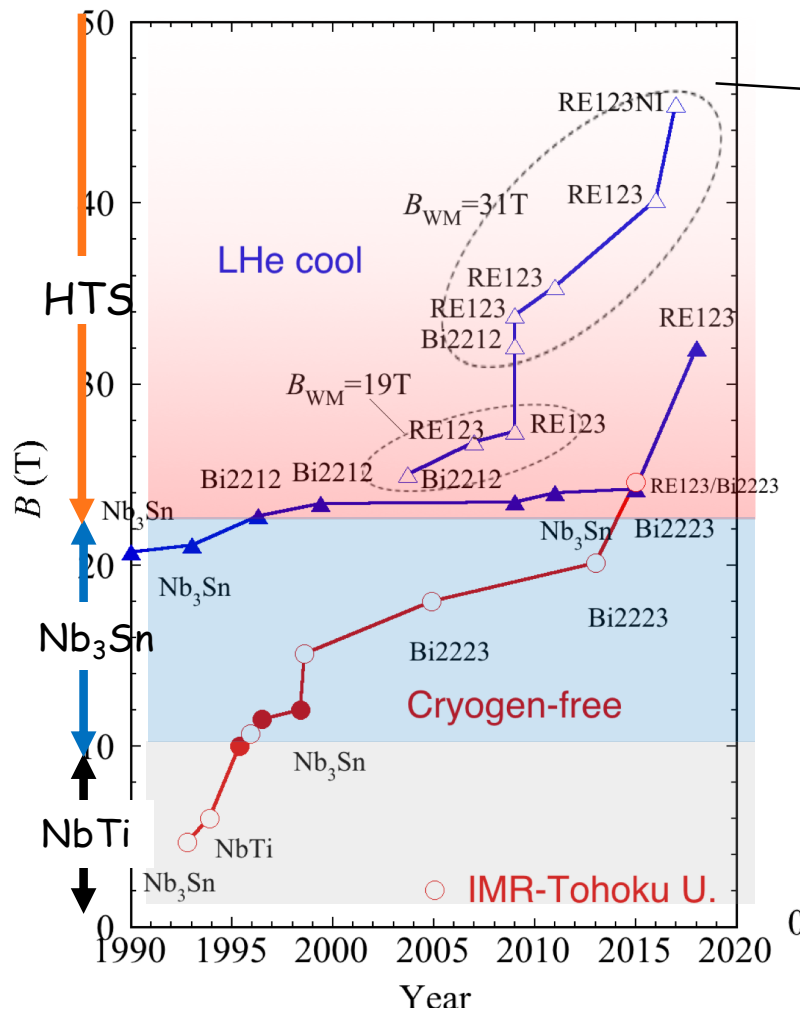
To develop high field superconducting magnet



High Field SC Magnet Developments - Practical Magnets -



High Field SC Magnet Developments - Practical Magnets + Demonstrations -



45.46 T- 14mm(NHMFL)

S. Hahn et al., Nature 570 (2019) 497.

Superconducting magnet beyond 40T can be targeted.

On going projects

- 40T-SM project (NHMFL)
- 1.3GHz (30.5T)NMR project (RIKEN)
- 30T-CSM (upgrade of 25T-CSM) (Tohoku U.)

etc



High Field HTS Magnets (All SC magnet)

S. Awaji, School Textbook "High Temperature Superconductors (in Japanese) vol. 2", JSAP, 2019 in press

Name	Group	Purpose	B(T) (HTS/LTS)	HTS	J_{con} (A/mm ²)	Max Stress (MPa)	ID (mm)	T _{op} (K)	Winding	Impregnation	Status	Year	Ref	
32T-SM	NHMFL	User magnet	32 (17/15)	RE123	193	378	40	4.2 (LHe)	DP	Dry	Open soon	2017	[1]	Insulated
25T-CSM	Tohoku U.	User magnet	24.6 (10.6/14)	Bi2223	150	323	96	4-8	DP	Epoxy/ turn separation	Open since 2016	2016	[2]	Insulated
20T-CSM	Tohoku U.	User magnet	20.1 (4.45/15.6)	Bi2223	118	212	90	4-6	DP	Epoxy/ turn separation	Open since 2013	2013	[3]	Insulated
1020MHz-NMR	NIMS /RIKEN	NMR	24.2 (3.62/20.4)	Bi2223	150	194	78	1.8 (LHe)	Layer	Wax	Obtained NMR signal, Closed in 2017	2016	[4]	Insulated
Fly-wheel	Furukawa	300kW FW	3.4	RE123	130		120	30-50	DP	Dry	Operate since 2015 as FW (4ton)	2015	[5]	Insulated
5T R&D	Fujikura	Demo	5	RE123	83	150	260	25	SP	Epoxy	Use at Fujikura	2013	[6]	Insulated
27T	IEE/CAS	Demo	27.2	RE123	389		36	4.2 (LHe)	NI-DP	Wax	NI	2019	[17]	NI
24T R&D	NIMS /RIKEN	Demo	24 (6.8/17.2)	RE123	428	408	50	4.2 (LHe)	Layer	Wax		2012	[7]	Insulated
25T R&D NMR	U. Geneva	Demo	25 (4/21)	RE123	733	139	20	2.2	Layer	Epoxy		2019	[8]	
3T-MRI	Mitsubishi	MRI	3	RE123	257		320	7	DP	Epoxy/ turn separation	Obtained MRI Image	2017	[9]	Insulated
9.4T-CSM	Toshiba	Demo	13.5	RE123	375	255	50	10	SP	Epoxy		2016	[10]	Insulated
NOUGAT	LNCMI/CEA-Saclay	Demo	14.5	RE123	717	(454@30T)	50	4.2(LHe)	DP	Dry	32.5T under 18T by resistive magnet	2019	[11]	MI
LBC	NHMFL	Demo	14.5	RE123	1420	691	14	4.2K(LHe)	SP	Dry	Damaged at 45.5T under 31T by resistive magnet	2017	[12]	NI
28T Demo	RIKEN	Demo	27.7 (6.3/4.3/17.1)	RE123 /Bi2223	396/238		40	4.2 (LHe)	Layer	Wax	Quench and damaged at 27.7T	2016	[13]	Insulated
30.5T	MIT	NMR	30.5 (18.8/11.7)	RE123	547		91	4.2 (LHe)	NI	Epoxy/ turn separation	NI, HTS coils damaged in test	2018	[14]	NI
25T-CSM	Tohoku U.	User magnet	24 (10/14)	RE123	221	407	104	4-8	SP	Epoxy/ turn separation	Quench and damaged at 24T	2015	[2]	Insulated
25T NI	SuNAM /MIT	Demo	26.4	RE123	404	286	35	4.2 (LHe)	NI-SP	Dry?	NI	2016	[15]	NI
25T	IEE/CAS	Demo	25.7 (10.7/15)	RE123	100-306	382	36	4.2 (LHe)	NI-DP	Wax	NI, Quench at 25.7T	2017	[16]	NI
3T-MRI	NIMS /SEI	MRI	3	Bi2223	114	137	514 (RT bore)	14	DP	Epoxy	MRI image at 1.5T, damaged in test	2013	[18]	Insulated

Practical use

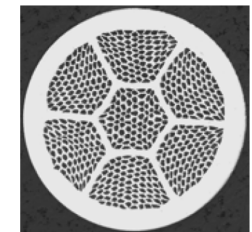
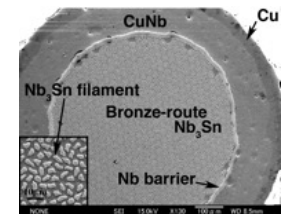
Demonstration

Damaged



From a viewpoint of magnet application 1

- Nb₃Sn
 - Non-Cu J_c is improving with the improvement of phase formation and an introduction of additional pinning centers
 - A mechanical strength is still improving.
- Bi2212
 - Unique round wire.
 - High in-field J_c due to the in-plane alignment.
 - Improvement of mechanical properties is expected.
- Fe-based Superconductor
 - Low cost and small anisotropy
 - Good in-field J_c in high field
 - Performance is improving.





From a viewpoint of magnet application 2

- Bi2223

- The mechanical strength is improving with the reinforcement and pre-compression. It is still improving.
- Good homogeneity



- REBCO

- High performance of in-field J_c and mechanical properties.
- J_c increases with an introduction of APC.
- A thickness of Hastelloy is decreasing in order to increase non-Cu J_c .
- Local degradation due to the complex stress should be overcome.

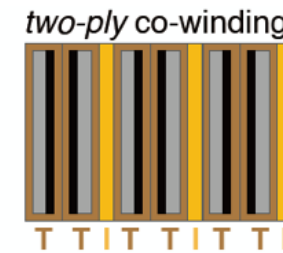
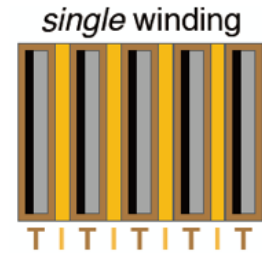




-View point of REBCO coil-

1. Bundles

- ✓ Current share at the local degradation
- ✓ Reduce fraction of insulation



2. Improve the stiffness of pancake coil

3. Protection from thermal runaway

- ✓ Dumping without thermal runaway (Passive protection).
- ✓ Dumping as fast as possible with normal states (Active protection using Q-heater)
- ✓ Non-insulation technique (Self protection)



As conclusion

- ✓ HTS wires have the ability to develop high field superconducting magnets beyond 20T.
- ✓ Key properties of high field superconductors are ...
in-field J_c and electromechanical properties.

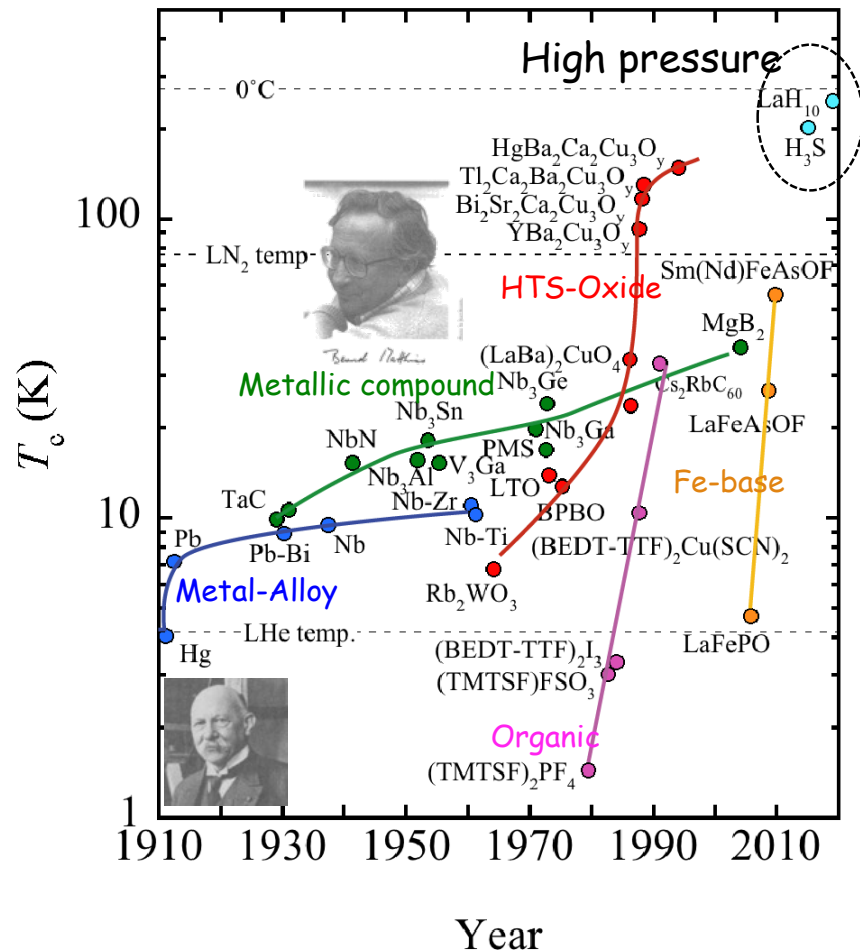


Generate a high magnetic field with toughness.

Develop 50T superconducting magnet!

Thank you for your kind attention!

Superconducting materials - Critical temperature T_c -



G. Bednorz, A. Müller,
LSCO, 1986



W. Wu, C. Chu YBCO, 1987



H. Maeda, BSCCO, 1988



Nagamatsu, Akimitsu,
MgB₂, 2000

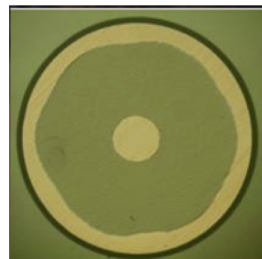


Kamihara, Hosono,
LaOFeP, 2006

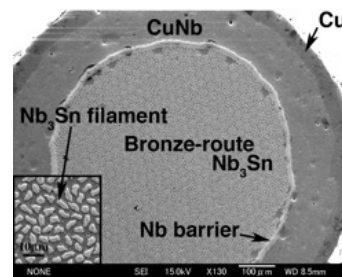


Practical Superconducting Wires

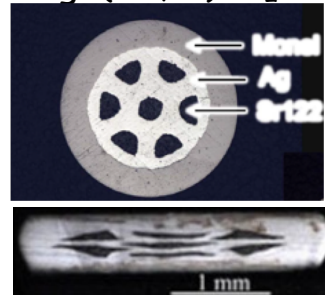
Cu/NbTi



$\text{Bz}-\text{CuNb}/(\text{Nb},\text{Ti})_3\text{Sn}$



$\text{Ag}/(\text{Sr}, \text{K})\text{Fe}_2\text{As}_2$



Ag/MgB_2

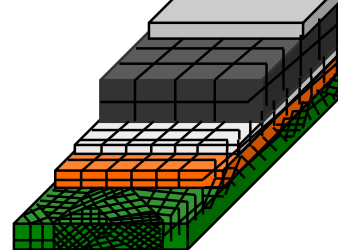
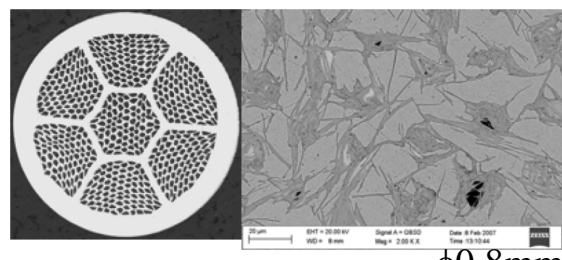


Brass/Ag/ $\text{Bi}_2\text{Sr}_2\text{Ca}_2\text{Cu}_3\text{O}_y$ (Bi2223) $\text{Ag}/\text{REBa}_2\text{Cu}_3\text{O}_y/\text{Hastelloy}$ (RE123, RE:rare earth)

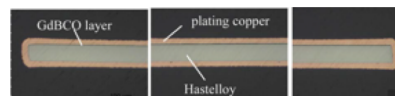


4mm x 0.2-0.3mm

$\text{Ag}/\text{Bi}_2\text{Sr}_2\text{Ca}_1\text{Cu}_2\text{O}_y$ (Bi2212)



Stabilization layer	Ag	5-50 μm
Superconducting layer	REBCO	1-2 μm
Buffer layer	PLD- CeO_2	0.4 μm
Buffer layer	IBAD- $\text{MgO}/\text{Gd}_2\text{Zr}_2\text{O}_7$	0.7 μm
Substrate	Hastelloy C276	25-100 μm





References

- [1] W. D. Markiewicz, D. C. Larbalestier, H. W. Weijers, A. J. Voran, K. W. Pickard, W. R. Sheppard, J. Jaroszynski, A. Xu, R. P. Walsh, J. Lu, A. V. Gavrilin, and P. D. Noyes, IEEE Trans. Appl. Supercond., 22 (2012) 4300704.
- [2] S. Awaji, K. Watanabe, H. Oguro, H. Miyazaki, S. Hanai, T. Tosaka, S. Ioka, Supercond. Sci. Technol. 30 (2017) 065001.
- [3] S. Awaji, H. Oguro, K. Watanabe, S. Hanai, S. Ioka, H. Miyazaki, M. Daibo, Y. Iijima, T. Saito and M. Itoh, Adv. Cryo. Eng. 59 (2014) 732.
- [4] G. Nishijima, TEION KOGAKU (J. Cryo. Super. Soc. Jpn.), 51 (2016) 329 (in Japanese).
- [5] T. Yamashita, M. Ogata, H. Matsue, Y. Miyazaki, M. Sugino, K. Nagashima, RTRI REPORT, 31 (2017) 47 (in Japanese).
- [6] M. Daibo, S. Fujita, M. Haraguchi, H. Hidaka, Y. Iijima, M. Itoh, T. Saito, TEION KOGAKU (J. Cryo. Super. Soc. Jpn.), 48 (2013) 226 (in Japanese).
- [7] S. Matsumoto, T. Kiyoshi, A. Otsuka, M. Hamada, H. Maeda, Y. Yanagisawa, H. Nakagome, H. Suematsu, Supercond. Sci. Technol. 25 (2012) 025017.
- [8] C. Barth, P. Komorowski, P. Vonlanthen, R. Herzog, R. Tediosi, M. Alessandrini, M. Bonura and C. Senatore, Supercond. Sci. Technol. 32 (2019) 075005.
- [9] S. Yokoyama, H. Miura, T. Matsuda, T. Inoue, Y. Morita, S. Otake, S. Sato, TEION KOGAKU (J. Cryo. Super. Soc. Jpn.), 52 (2013) 217 (in Japanese).
- [10] H. Miyazaki, S. Iwai, T. Uto, Y. Otani, M. Takahashi, T. Tosaka, K. Tasaki, S. Nomura, T. Kurusu, H. Ueda, S. Noguchi, A. Ishiyama, S. Urayama, H. Fukuyama, IEEE Trans. Appl. Supercond., 27 (201) 4701705.
- [11] Private communication, EUCAS2019 3-LO-HH-025, MT26 Fri-Mo-Or27-04.
- [12] S. Hahn, K. Kim, K. Kim, X. Hu, T. Painter, I. Dixon, S. Kim1, K R. Bhattacharai, S. Noguchi, J. Jaroszynski. D. C. Larbalestier1, Nature, 570 (2019)496.
- [13] Y. Yanagisawa, K. Kajita, S. Iguchi, Y. Xu, M. Nawa, R. Piao, T. Takao, H. Nakagome, M. Hamada, T. Noguchi, G. Nishijima,
- [14] Y. Iwasa, J. Bascuñán, S. Hahn, J. Voccio, Y. Kim, T. Lécrevisse, J. Song, K. Kajikawa, IEEE Trans. Appl. Supercond., 25 (2015) 4301205.
- [15] S. Yoon, J. Kim, K. Cheon, H. Lee, S. Hahn, S. H. Moon, Supercond. Sci. Technol. 29 (2016) 04LT04.
- [16] J. Liu, Q. Wang, Y. Dai, L. Wang, L. Qin, K. Chang, L. Li, B. Zhao, IEEE/CSC & ESAS SUPERCONDUCTIVITY NEWS FORUM (global edition), July 2016
- [17] Private communication, EUCAS2019
- [18] Y. Terao, O. Ozaki, S. Kawashima, K. Saito, T. Hase, H. Kitaguchi, K. Sato, S. Urayama, H. Fukuyama., IEEE Trans. Appl.d Supercond. 24 (2014) 1.